Non-Abelian magnetic field and curvature effects on pair production

S. Kürkçüoğlu[1,*] B. Özcan[1,†] and G. Ünal[2,‡]

[1]*Middle East Technical University, Department of Physics, Dumlupınar Boulevard, 06800 Ankara, Turkey*
[2]*Faculty of Engineering, Başkent University, 06790 Ankara, Turkey*

We calculate the Schwinger pair-production rates in $\mathbb{R}^{3,1}$ as well as in the positively curved space $S^2 \times \mathbb{R}^{1,1}$ for both spin-0 and spin-$\frac{1}{2}$ particles under the influence of an external $SU(2) \times U(1)$ gauge field producing an additional uniform non-Abelian magnetic field besides the usual uniform Abelian electric field. To this end, we determine and subsequently make use of the spectrum of the gauged Laplace and Dirac operators on both the flat and the curved geometries. We find that there are regimes in which the purely non-Abelian and the Abelian parts of the gauge field strength have either a counterplaying or reinforcing role, whose overall effect may be to enhance or suppress the pair-production rates. Positive curvature tends to enhance the latter for spin-0 and suppress it for spin-$\frac{1}{2}$ fields, while the details of the couplings to the purely Abelian and the non-Abelian parts of the magnetic field, which are extracted from the spectrum of the Laplace and Dirac operators on S^2, determine the cumulative effect on the pair-production rates. These features are elaborated in detail.

I. INTRODUCTION AND SUMMARY OF RESULTS

Elucidating the nonperturbative effects in quantum field theories is an important area of research on which considerable contemporary efforts are focused. Problems in this context include a variety of phenomena, some of which are both conceptually and computationally very difficult and usually escape a fully satisfactory theoretical description, such as the confinement of quarks in QCD. Nevertheless, there are also more tractable problems such as the Casimir effect [1] and Schwinger pair production [2]. Although both of these phenomena are conceived as vacuum effects in QED, the former has already been verified in several different direct experiments over the past few decades, while it has not been possible to observe the latter, as the amplitude for the production of massive particle and antiparticle pairs is exponentially suppressed with $e^{-m^2\pi/E}$ and requires a very strong electric field $\approx 10^{18}$ V m^{-1}, while it is expected that the recent technological advances can open new avenues for exploring QED in intense background fields [3,4].

There have been continual efforts ever since the original work of Schwinger [2] (and the important earlier works due to Sauter [5] and Euler and Heisenberg [6]) to look for alternative mechanisms as well as novel aspects and features that may enhance the effect and thereby reduce the electric field strength required for its observation. Time-dependent electric fields tend to enhance the pair-production amplitudes at a significant rate [7–9]; nevertheless, experiments conducted using high-intensity laser beams have not, so far, led to an observational confirmation (see, for instance, [4] and the references therein). Effects of inhomogenous electric fields are also addressed in several papers [10–12] ([13] provides a comprehensive review). Very recently, it has been reported that a condensed matter analog involving electrons and holes is observed at the Dirac point of graphene superlattices [14] and ballistic graphene transistors [15].

Another possible route to search for enhancement effects, which was not explored up until very recently, is to consider physical configurations that allow the produced pairs to be in bound quantum states as opposed to being free, with the expectation that the bound state spectrum of the relevant gauged differential operator in the effective action helps to effectively ease the suppression due to nonvanishing mass. Gravitational and magnetic background fields can provide such physical configurations with charge symmetric binding and with this motivation, in two recent papers [16,17], in which one of the present authors (S. K.) is a coauthor, possible influences of an additional uniform Abelian magnetic field as well as constant positive and negative curvature are considered by computing the pair-production amplitudes in the Minkowski space and the product manifolds $S^2 \times \mathbb{R}^{1,1}$ and $H^2 \times \mathbb{R}^{1,1}$. Results of these papers

indicated a decrease for spin 0 and increase for spin $\frac{1}{2}$ for the pair-production amplitudes with the applied magnetic field, while positive curvature enhanced the effect for spin 0 and suppressed it for spin $\frac{1}{2}$, and the opposite prevailed for the negative curvature. For spin-1 particles, which were treated as a part of an $SU(2)$ gauge field, it was found that the pair-production rate increases with the applied magnetic field, while the positive (negative) curvature acts to suppress (enhance) the effect [17].

In the present work, we continue along this line of development and explore the effects of additional uniform non-Abelian $SU(2) \times U(1)$ magnetic gauge field backgrounds[1] on the pair production of spin-0 and spin-$\frac{1}{2}$ fields on flat as well as positively curved backgrounds, i.e., in the Minkowski space $\mathbb{R}^{3,1}$ and the product manifold $S^2 \times \mathbb{R}^{1,1}$, where $U(1)$ provides the usual uniform magnetic field in both cases. We assume that both the scalar and spinor fields are also charged under the $SU(2)$ part of the gauge field background, and, to distinguish this from the usual spin, we refer to it as the "isospin" degree of freedom, alluding to the similar uses of the latter terminology in the literature [19–21]. There are a number of motivations to consider a uniform non-Abelian $SU(2) \times U(1)$ magnetic background which we would like to stress at this stage. First of all, for both spin-0 and $-\frac{1}{2}$ particles and in both of the background geometries, the energy spectrum is still quantized, and, hence, the produced pairs fill bound states,[2] and we may expect enhancement in pair-production amplitudes due to the reasons we have stated in the previous paragraph. Our models also provide novel and fully tractable examples in which effects of the external uniform Yang-Mills fields are completely incorporated in the pair-production amplitudes, given the scarcity of research in exploring this aspect of the effect apart from a few papers published a long time ago and limited to only the flat geometry [18,22]. Another compelling source of motivation derives from the recent advances in condensed matter physics. For instance, cold atomic gases subjected to time-dependent potentials can be described by the presence of external artificial Abelian and non-Abelian gauge fields [23–25]. Also, two-dimensional electron gases in the presence of Rashba [26] and/or Dresselhaus [27] type of spin-orbit coupling terms can be described as electrons exposed to external

non-Abelian magnetic fields [28–31]. Considering these facts together with the aforementioned pair production like effects in graphene superlattices and transistors [14,15], there may perhaps be viable routes to experimentally explore the possible influences of such artificial non-Abelian fields on analogs of pair-production-type occurrences in condensed matter systems in the foreseeable future.

Another quite interesting motivation for studying the effects of curvature on pair production is our approach's possible connections with the recent results reported in [32], which develops a unified description of Schwinger effect and a novel gravitational particle production mechanism based on the heat kernel expansion of the one-loop effective action. For instance, the authors of [32] compute the particle production rates due to a real scalar field in a Schwarzschild background without explicitly invoking the presence of a event horizon.[3] In [34], these results of [32] are conjectured to be related to the conformal (trace) anomaly, with the pair-production rates being proportional to the anomalous trace of the energy-momentum tensor of the relevant matter fields in the gravitational and/or electromagnetic backgrounds. We think that investigating any possible connections of the results of our present paper as well those of [16,17] with the aforementioned developments provided in [32,34] may lead to a broader perspective in understanding the different facets of particle production effects in quantum field theories.

For the spherical geometry, it is important to emphasize the fundamental role played by the total angular momentum operators $\vec{J} = \vec{L} + \frac{\vec{\sigma}}{2}$ and $\vec{K} = \vec{L} + \frac{\vec{\sigma}}{2} + \frac{\vec{\tau}}{2}$, for spin-0 and $-\frac{1}{2}$ particles, respectively, where $\vec{L}$ stands for the orbital angular momentum of the charge-Dirac monopole system and $\frac{\vec{\tau}}{2}$ and $\frac{\vec{\sigma}}{2}$ generate the spin and isopin degrees of freedom, respectively. As clearly demonstrated in Appendices C and D, the spectrum of their associated quadratic Casimir operators is critical in obtaining the energy spectrum of the spin-0 and $-\frac{1}{2}$ fields, without which the results presented in this paper for the pair-production amplitudes could not have been obtained. In other words, we may state that the isometry group of S^2 being also $SO(3) \approx SU(2)$ is compatible with the isospin to form the "total" isometry operator $\vec{J}$ acting on the space and gauge degrees of freedom altogether. This brings us to recognize an important difference between the positively and negatively curved background geometries. As we have already pointed out above, constant negative curvature background is equally as interesting as the positively curved one, and as presented in [16] pair-production amplitudes on $H^2 \times \mathbb{R}^{1,1}$ lead to reversed enhancement or suppression effects between spin-0 and $-\frac{1}{2}$ fields compared to those on $S^2 \times \mathbb{R}^{1,1}$. Nevertheless, at least with the approach used in this paper, it does not appear possible to obtain the energy spectrum of the particles

---

[1]We may note that this configuration is distinct from that treated in [18], where a component of the uniform $SU(2)$ field strength could be of electric type and could cause the decay of the vacuum by pair production.

[2]We also explore the limiting situation in which the Abelian magnetic charge vanishes, which effectively reduces the magnetic background to a pure $SU(2)$ field. In this case, the energy spectra for spin-0 and $-\frac{1}{2}$ particles in the flat background become continuous, while they remain quantized in the spherical background.

[3]Applicability of the results of [32] to any gravitational field is being contested in a recent paper [33].

on H^2 in an $SU(2) \times U(1)$ background, since the isometry group of H^2 being $SO(2,1) \simeq SU(1,1)$ cannot be combined together with the isospin generators, which are spanning an $SU(2)$, to form operators of the form $\vec{J}$ and/or $\vec{K}$, which can be exploited to calculate the energy spectra.[4][5]

To compute the pair-production amplitudes, we make use of the spectrum of the gauged Laplacians on $\mathbb{R}^2$ and S^2, which are already available in [28], while we derive those for the square of the Dirac operators for both of the geometries. The latter are interesting problems in their own right with several intriguing and novel features, which includes a detailed account of their zero modes, and we provide a comprehensive analysis. A brief summary of our results is as follows. Because of the isospin degree of freedom, the energy spectrum splits into two branches, namely, $\Lambda_{n_1}^+(\beta')$ and $\Lambda_{n_1}^-(\beta')$ for the scalar and $\lambda_{n_1}^+(\beta')$ and $\lambda_{n_1}^-(\beta')$ spinor fields.[6] In the flat geometry, similar to the case of the pure uniform Abelian magnetic field [16], pair production is, in general, suppressed for spin-0 and enhanced for spin-$\frac{1}{2}$ fields with increasing non-Abelian magnetic field β' (this is the non-Abelian field strength β scaled by the square root of the Abelian field B_1, i.e., $\beta' = \frac{\beta}{\sqrt{B_1}}$, as will be defined in the next section). These outcomes are mainly being due to monotonic increase of

$\Lambda_{n_1}^+(\beta')$ with β', which makes the corresponding states harder to fill by the produced particle-antiparticle pairs due to higher energy cost in the former (spin-0) and due to the proliferation of zero energy states $\lambda_0^-(\beta')$ with increasing degeneracy in the latter[7] (spin-$\frac{1}{2}$ case). However, there are also some very novel features. For spin-0 fields, for a certain range of values of β', $\Lambda_{n_1}^-(\beta')$ becomes less than its value at $\beta' = 0$, and, therefore, the corresponding levels are less energy costly to get filled. This leads to the pair-production rates, which exceed those at $\beta' = 0$ at sufficiently large values of $y = \frac{B_1}{E}$. For $\beta' < \beta'_{c_1}$, these rates increase further with increasing β, while they decrease with it for $\beta'_{c_1} < \beta' < \beta'_{c_2}$, with the estimates for the critical β' values provided in Sec. II. For spin-$\frac{1}{2}$ particles, we find that, for sufficiently small values of $y = \frac{B_1}{E}$, pair-production rates are further enhanced, since $\lambda_0^-(\beta')$ monotonically decreases toward $\lambda_0^-(\beta' = 0) = 0$ with β', making the corresponding eigenstates effectively degenerate with the zero energy states. Nevertheless, as $y = \frac{B_1}{E}$ increases, pair-production rates converge back to that at $\beta' = 0$, since $\lambda_0^+(\beta')$ increases monotonically with β' and states with corresponding energies become energetically costly to be filled, counterbalancing the effect of the former. All of these features are elaborated in detail in Sec. II.

In the curved geometry $S^2 \times \mathbb{R}^{1,1}$, very novel features are encountered as the continuous parameter α governing the non-Abelian field strength varies, leading to either a competition with or further support of the effect (which may be to enhance or suppress the relative pair-production (RPP) rates as discussed in [16] and already mentioned above) of the quantized Abelian magnetic field. For scalar fields, two critical values of α, which are determined in terms of the Dirac monopole charge N, govern the RPP rates between the curved and flat backgrounds. The latter is measured via the function $\gamma_0(\omega, \alpha, N)$, which is defined in Sec. III. For $0 < \alpha < \alpha_{c_1}$, $\gamma_0(\omega, \alpha, N) > 1$, and it indicates relatively larger pair production in the curved space, which tends to converge to the flat space results with increasing N. For $\alpha_c^{(1)} < \alpha < \alpha_c^{(2)}$, $\gamma_0(\omega, \alpha, N)$ is slightly above the value 1 roughly within the interval $0 < \omega \lesssim 1$ (i.e., large electric field or small curvature) but eventually goes below it as ω is increased further, while we again find $\gamma_0(\omega, \alpha, N) > 1$ for $\alpha > \alpha_c^{(2)}$, indicating an increasing RPP. Another critical value of α, namely, $\alpha_c^{(3)} = \frac{1}{2}(1 + \sqrt{2N+1})$, facilitates the comparison of the pair-production amplitudes with and without the non-Abelian field (i.e., $\alpha \neq 0$ and $\alpha = 0$), which is measured using the function $R_0(\omega, \alpha, N)$, which will also be defined in Sec. III. We find that, at large ω,

---

[4]One possible route to evade these difficulties encountered on H^2 may be to consider higher-dimensional noncompact spaces, such as $H^n = \frac{SO(n,1)}{SO(n)}$, and gauge the invariant subgroup $SO(n)$ or a subgroup $K \supset SO(n)$, i.e., to consider magnetic backgrounds valued in the Lie algebra of K, in which the spectrum of gauged Laplacians and Dirac operators may be obtained at least at certain values of the coupling constants from pure group theoretical considerations analogous to those used in solving Landau problem in higher dimensions [35]. Since this is beyond the scope of our present work, we do not pursue it here any further.

[5]In analogy with the gauge potential $\alpha \frac{\vec{r} \times \vec{\omega}}{a^2}$ (C3) on S^2 and using the isometrical embedding of H^2 in $R^{2,1}$ with the metric $(+,+,-)$, it may be tempting to consider $A_{\text{non-Abelian}}^\mu = \frac{1}{a^2} \varepsilon^{\mu\nu\rho} r_\nu \omega_\rho$, where $-a^2 = x^2 + y^2 - z^2$, $[\omega_\mu, \omega_\nu] = 2i\varepsilon_{\mu\nu\rho}\omega^\rho$, and $\vec{\omega} = (i\sigma_1, i\sigma_2, \sigma_3)$ are 2×2 matrices spanning the two-dimensional irreducible representation (IRR) of $SU(1,1)$. $\vec{\omega}$ is not a Hermitian basis, since it spans a finite-dimensional IRR of $SU(1,1)$, which is noncompact. Although it is possible to define the "total" isometry operator valued in $su(1,1)$, to study the spectrum of its associated quadratic Casimir operator one would have to work out the tensor products of infinite-dimensional unitary IRRs (with $\vec{L}$ belonging either to the principal continuous or one of the discrete series) and the two-dimensional IRR in which $A_{\text{non-Abelian}}^\mu$ taken. Thus, it becomes quite cumbersome to determine the spectrum of the gauged Laplacian on H^2, if not completely nontractable. Incidentally, it may be noted that, on higher-dimensional spaces such as ultrahyperboloids, it is possible to obtain the spectrum of Laplacians gauged under noncompact groups [36].

[6]Let us remark that the corresponding wave functions for $\Lambda_{n_1}^\pm(\beta')$ and $\lambda_{n_1}^\pm(\beta')$ are not the eigenfunctions of the isospin as explained in Appendices A and B.

[7]Here, we should either conceive the uniform magnetic field to be over a finite portion of the space or introduce an infrared cutoff via a mass term. We use the latter option in this paper, as will be discussed in the ensuing sections.

$R_0(\omega, \alpha, N) \to \infty, \frac{1}{2}\frac{N+2}{N+1}, 0$, for $\alpha <, =, > \alpha_c^{(3)}$, indicating enhanced, saturated, and suppressed pair-production amplitudes, respectively. We also see $R_0(\omega, \alpha_c^{(3)}, N)$ converging to $\frac{1}{2}$ at large N and matching with the result we obtained in the flat background. For the spinor fields, the RPP is measured via the function $\gamma_{1/2}(\omega, \alpha, N)$, and, in general, it is less than 1 and becomes more so with increasing α indicating a decrease in RPP as the non-Abelian magnetic field becomes stronger. This is countered by the restoring effect of the zero modes, whose degeneracy grows with increasing Dirac monopole charge N and drives the $\gamma_{1/2}(\omega, \alpha, N)$ back to 1 and the pair-production rates to those found in the flat background. Nevertheless, the overall effect is still larger for $\alpha \neq 0$ compared to $\alpha = 0$, since the lowest-lying energies that follow after zero modes in the spectrum remain below their value at $\alpha = 0$ and the corresponding states are, therefore, more eligible to get filled by the produced pairs. Increasing N or ω counteracts, as in either case the dominance of the zero modes is elevated and the pair-production rates converge to their vales at $\alpha = 0$.

Finally, the case of a vanishing Abelian magnetic field (that is, the presence of a pure uniform $SU(2)$ magnetic field) is also studied for the scalar and the spinor fields in both the flat and the curved backgrounds, and the results are compared and contrasted with those summarized above.

II. PAIR-PRODUCTION RATES FOR SCALAR FIELDS FIELDS ON $\mathbb{R}^{3,1}$

In this section, we calculate the pair-production rate for particles with spin 0 in the Minkowski space $\mathbb{R}^{3,1}$, under the influence of uniform Abelian and non-Abelian fields. In addition to a uniform electric field $\vec{E} = E\hat{x}_3$ in the x_3 direction as usual, we consider an additional $SU(2) \times U(1)$ gauge field generating a uniform magnetic field as we shall introduce shortly. In order to obtain the pair-production rates, our strategy is to Wick rotate $\mathbb{R}^{3,1}$ to $\mathbb{R}^4 = \mathbb{R}^2 \times \mathbb{R}^2$ and evaluate the Euclidean effective action due to appropriately constructed gauged Laplacian and Dirac operators for spin-0 and spin-1/2 particles, respectively. On the first $\mathbb{R}^2$ copy, spanned by (x_1, x_2) coordinates, we introduce the $SU(2) \times U(1)$ gauge field of the form

$$\vec{A}_{(1)} = \frac{B_1}{2}(-x_2\hat{x}_1 + x_1\hat{x}_2)\mathbb{1}_2 + \beta(-\sigma_2\hat{x}_1 + \sigma_1\hat{x}_2), \quad (2.1)$$

where $\vec{\sigma} := (\sigma_1, \sigma_2, \sigma_3)$ are the usual Pauli matrices. Clearly, $\vec{A}$ is composed of a $U(1)$ gauge field $\vec{A}^{U(1)} := \frac{B_1}{2}(-x_2\hat{x}_1 + x_1\hat{x}_2)$ and a purely $SU(2)$ gauge field $A_i^{SU(2)} := -\beta\epsilon_{ij}\sigma_j$, where $i, j = 1, 2$. In what follows, we will call this $SU(2)$ field (as well as its analog on S^2 to be introduced in Sec. III) as the "isospin" gauge field to distinguish it from the usual spin, which will naturally be present in the ensuing

discussion for spin-1/2 particles. We can easily see that $\vec{A}$ generates a uniform magnetic field

$$F_{12} = B_1\mathbb{1}_2 + 2\beta^2\sigma_3. \quad (2.2)$$

On the second $\mathbb{R}^2$ copy spanned by (x_3, x_4), we consider another $U(1)$ gauge field, say, $\vec{A}_{(2)}$, generating a uniform Abelian magnetic field $F_{34} := B_2$. We can take $\vec{A}_{(2)}$ in the Landau or in the symmetric gauge, but this is going to be immaterial for our purposes. The magnetic field B_2 will be Wick rotated to the uniform electric field ($F_{34} \to iF_{03}$, i.e., $B_2 \to iE$) at an appropriate stage in the calculation (to be given below), and the sole purpose to introduce it at this stage is to take advantage of the well-known solution of the Landau problem to write down the spectrum of the gauged Laplacian and Dirac operators to facilitate the evaluation of the Euclidean effective actions. Thus, the total gauge field on $\mathbb{R}^4$ is $A_\mu := (\vec{A}_{(1)}, \vec{A}_{(2)})$, and Wick rotating $\mathbb{R}^4$ to $\mathbb{R}^{3,1}$, i.e., $(x_1, x_2, x_3, x_4) \to (x_1, x_2, x_3, -ix_0)$, yields the electric and the magnetic fields $\vec{E} = E\mathbb{1}_2\hat{x}_3$ and $\vec{B} = F_{12}\hat{x}_3$, respectively (with the $U(1)$ accounting for the electromagnetic field).

A. Spectrum of the gauged Laplacian

Introducing the covariant derivative $D_\mu := \partial_\mu - iA_\mu$ on $\mathbb{R}^4$ ($\mu : 1, 2, 3, 4$), gauged Laplace operator on $\mathbb{R}^4$ may be written in a self-evident notation as

$$-D^2 = -(D_{(1)}^2 + D_{(2)}^2)$$
$$= -(\vec{\partial} - i\vec{A}_{(1)})^2 - (\vec{\partial} - i\vec{A}_{(2)})^2. \quad (2.3)$$

$-D_{(1)}^2$ can be expressed in the form

$$-D_{(1)}^2 = 2B_1\left(a^\dagger a + \sqrt{2}\beta'(a^\dagger\sigma_+ + a\sigma_-) + \frac{1}{2}(1 + 2\beta'^2)\mathbb{1}_2\right), \quad (2.4)$$

where a and $a^\dagger$ are the annihilation and creation operators, respectively, defined in the same manner as in the Landau problem (see Appendix A) and $\sigma_\pm = \sigma_1 \pm i\sigma_2$ are the isospin ladder operators. Here, we have also introduced the notation $\beta' = \beta/\sqrt{B_1}$ as the dimensionless non-Abelian magnetic field strength by scaling β with respect to the square root of the Abelian magnetic field. This operator is essentially very similar to the Hamiltonian of the Jaynes-Cummings model [37] as is already discussed in [28], and it can easily be diagonalized. Its spectrum is

$$\Lambda_{n_1}^\pm = 2B_1\left(n_1 \pm \sqrt{2\beta'^2 n_1 + 1/4 + \beta'^2}\right), \quad (2.5)$$

where $n_1 = 0, 1, 2\ldots$ for the upper and $n_1 = 1, 2, \ldots$ for the lower signs, respectively. Details of a straightforward

calculation leading to (2.5) is provided in Appendix A for convenience. Note, in particular, that the lowest-lying state is given by $\Lambda_0^+ = 2B_1(\beta'^2 + 1/2)$.

On the other hand, the spectrum of $-D_{(2)}^2$ is nothing but the solution of the Landau problem, and the eigenvalues are $B_2(2n_2 + 1)$, where $n_2 = 0, 1, 2, \ldots$ Putting these facts together, we have

$$\text{Spec}(-D^2 + m^2) = \Lambda_{n_1}^\pm + B_2(2n_2 + 1) + m^2, \quad (2.6)$$

with the density of states given as $\frac{B_1}{2\pi} \times \frac{B_2}{2\pi}$, since the presence of the non-Abelian magnetic field does not alter the density of states corresponding to the spectrum $\Lambda_{n_1}^\pm$ of $-D_{(1)}^2$ as can readily be inferred from the calculations provided in Appendix A.

B. Pair-production rates

We start with the computation of the Euclidean effective action $\Gamma_E \equiv \text{Tr} \log(-D^2 + m^2)$, which we will Wick rotate to Lorentzian signature at an appropriate stage. Following the approach in [16], we have

$$\Gamma_E = -\text{Tr} \lim_{\epsilon \to 0} \int_\epsilon^\infty \frac{ds}{s} e^{-s(-D^2 + m^2)}$$

$$= -\lim_{\epsilon \to 0} \int_0^\infty d^4x \int_\epsilon^\infty \frac{ds}{s} \langle x | e^{-s(-D^2 + m^2)} | x \rangle. \quad (2.7)$$

Expanding the position kets $|x\rangle$ on $\mathbb{R}^4$ with respect to the eigenkets $|n_1, n_2, \alpha\rangle$ (with the auxiliary index α labeling the degeneracy) of the gauged Laplacian, we may write

$$\Gamma_E = -\lim_{\epsilon \to 0} \int_0^\infty d^4x \int_\epsilon^\infty \frac{ds}{s} \sum_{n_1, n_2, \alpha} \langle x | e^{-s(-D^2 + m^2)} | n_1, n_2, \alpha \rangle \langle n_1, n_2, \alpha | x \rangle$$

$$= -\lim_{\epsilon \to 0} \int_0^\infty d^4x \int_\epsilon^\infty \frac{ds}{s} \sum_{n_1, n_2, \alpha} \langle x | n_1, n_2, \alpha \rangle \left(e^{-s(\Lambda_{n_1}^+ + B_2(2n_2+1) + m^2)} + e^{-s(\Lambda_{n_1}^- + B_2(2n_2+1) + m^2)} \right) \langle n_1, n_2, \alpha | x \rangle$$

$$= -\lim_{\epsilon \to 0} \int_0^\infty d^4x \int_\epsilon^\infty \frac{ds}{s} \sum_{n_1, n_2, \alpha} \psi_{n_1, n_2, \alpha}^*(x) \psi_{n_1, n_2, \alpha}(x) \left(e^{-s(\Lambda_{n_1}^+ + B_2(2n_2+1) + m^2)} + e^{-s(\Lambda_{n_1}^- + B_2(2n_2+1) + m^2)} \right), \quad (2.8)$$

where $\psi_{n_1, n_2, \alpha}(x)$ denote the eigenfunctions of the gauged Laplacian in the position basis. Using the normalization of $\psi_{n_1, n_2, \alpha}(x)$ and the density of states $\frac{B_1 B_2}{(2\pi)^2}$, sum over these degenerate states can be performed,[8] and we may write

$$\Gamma_E = -\lim_{\epsilon \to 0} \int_0^\infty d^4x \int_\epsilon^\infty \frac{ds}{s} \frac{B_1 B_2}{(2\pi)^2} \sum_{n_1, n_2} \left(e^{-s(\Lambda_{n_1}^+ + B_2(2n_2+1) + m^2)} \right.$$

$$+ e^{-s(\Lambda_{n_1}^- + B_2(2n_2+1) + m^2)} \bigg)$$

$$= -\lim_{\epsilon \to 0} \int_0^\infty d^4x \frac{B_1}{8\pi^2} \int_\epsilon^\infty \frac{ds}{s^2} \frac{sB_2}{\sinh sB_2} \sum_{n_1} \left(e^{-s(\Lambda_{n_1}^+ + m^2)} \right.$$

$$+ e^{-s(\Lambda_{n_1}^- + m^2)} \bigg). \quad (2.9)$$

In the second line in (2.9), we have performed the summation over the index n_2. This is the appropriate stage to Wick rotate the Euclidean effective action via $x_4 \to ix_0$ and $B_2 \to -iE$ and identify Γ_E with iS_{eff}. The pair-production rate is proportional to the real part of the latter, which we denote as $\text{Re}(iS_{\text{eff}})$. We have

$$iS_{\text{eff}} = \frac{i}{8\pi^2} \lim_{\epsilon \to 0} \int_0^\infty d^4x B_1 \int_\epsilon^\infty \frac{ds}{s^2} \frac{sB_2}{\sinh sB_2} \sum_{n_1} \left(e^{-s(\Lambda_{n_1}^+ + m^2)} \right.$$

$$+ e^{-s(\Lambda_{n_1}^- + m^2)} \bigg). \quad (2.10)$$

We can now perform the s integration in the same manner as in [16]. The integral has singularities at $s = n\pi/E$, $n = 1, 2, 3, \ldots$. For the pair-production rate, we need only the real part of iS_{eff}, and the contributions to this come from the integrals around small semicircles at each singularity. Therefore, taking our integration variables as $s = n\pi/E + z$ with $|z| \ll 1$ and performing the integration over the parameter z, we get

$$\text{Re}(iS_{\text{eff}}) = \frac{EB_1}{8\pi^2} \int d^4x \sum_{n=1}^\infty \frac{(-1)^n}{n} \sum_{n_1} \left(e^{-(n\pi/E)(\Lambda_{n_1}^+ + m^2)} \right.$$

$$+ e^{-(n\pi/E)(\Lambda_{n_1}^- + m^2)} \bigg), \quad (2.11)$$

which, after performing the sum over n, can be cast into the form

$$\text{Re}(iS_{\text{eff}}) = \frac{EB_1}{8\pi^2} \int d^4x \sum_{n_1}$$

$$\times \ln\left(1 + e^{-(2\pi B_1/E)(n_1 + \sqrt{2\beta'^2 n_1 + 1/4} + \beta'^2 + \frac{1}{2}m^2)} \right)$$

$$+ \ln\left(1 + e^{-(2\pi B_1/E)(n_1 - \sqrt{2\beta'^2 n_1 + 1/4} + \beta'^2 + \frac{1}{2}m^2)} \right). \quad (2.12)$$

Introducing the dimensionless parameter $y := B_1/E$ and taking the limit $m^2 \to 0$, we are able to write

---

[8] $\int d^4x \sum_\alpha \psi_{n_1, n_2, \alpha}^*(x) \psi_{n_1, n_2, \alpha}(x) = \sum_\alpha 1 = \int d^4x \frac{B_1 B_2}{(2\pi)^2}$.

$$\mathrm{Re}(iS_{\mathrm{eff}}) = -\int d^4x \frac{E^2}{96\pi} f_0(y,\beta'), \tag{2.13}$$

where

$$
\begin{aligned}
f_0(y,\beta') &= \frac{12y}{\pi} \sum_{n=1}^{\infty} \frac{(-1)^{n+1}}{n} \sum_{n_1} \left(e^{-\pi n y \frac{\Lambda_{n_1}^+}{B_1}} + e^{-\pi n y \frac{\Lambda_{n_1}^-}{B_1}} \right) \\
&= \frac{12y}{\pi} \left(\sum_{n_1=0}^{\infty} \ln(1 + e^{-2\pi y(n_1 + \sqrt{2\beta'^2 n_1 + 1/4} + \beta'^2)}) + \sum_{n_1=1}^{\infty} \ln(1 + e^{-2\pi y(n_1 - \sqrt{2\beta'^2 n_1 + 1/4} + \beta'^2)}) \right).
\end{aligned}
\tag{2.14}
$$

We see that $f_0(y,\beta') \to 1$ as $y \to 0$, i.e., for $B_1 \to 0$ and $\beta \to 0$ with $\beta' = \frac{\beta}{\sqrt{B_1}}$ held fixed.[9] Then, (2.13) yields nothing but twice the usual Schwinger result in this limit, the overall factor of 2 being due to equal contributions from isospin up and down degrees of freedom in this limit.

In order to assess the pair-production rates in this setting, we may inspect the behavior of the function $f_0(y,\beta')$ as we vary y at various values of β'. In Fig. 1(a), the profile of this function is plotted for $\beta' = 0, 1/4, 1/2, \sqrt{\frac{3}{8}}, 7/8, 1, 3/2$. We immediately observe that $f_0(y,\beta')$ decreases with increasing y. This means that with the increasing Abelian field strength, B_1 ($y = B_1/E$) leads to a decrease in the pair-production rates. This feature of the function $f_0(y,\beta')$ is expected and in accord with the case studied in [16] with a purely Abelian magnetic field. In fact, we observe that the eigenvalues $\Lambda_{n_1}^+(\beta')$ are always larger than $\Lambda_{n_1}^+(\beta' = 0) = 2B_1(n_1 + \frac{1}{2})$ (i.e., those obtained for the purely Abelian magnetic field) and become larger with increasing β', too. We conclude that these quantum states become increasingly harder to be filled by particle-antiparticle pairs as β' increases, and we observe a significant decrease in the value of the function $f_0(y,\beta')$ for increasing β' values. However, for a given level n_1, $\Lambda_{n_1}^-(\beta')$ starts with the value $\Lambda_{n_1}^-(\beta' = 0) = 2B_1(n_1 - \frac{1}{2})$ at $\beta' = 0$, decreases to the minimum $2B_1 \frac{n_1^2 - 1/4}{2n_1}$ at $\beta'_{c_1} = \sqrt{\frac{n_1^2 - 1/4}{2n_1}}$, and monotonically increases starting from this point and attains $2B_1(n_1 - \frac{1}{2})$ value again at $\sqrt{2n_1 - 1}$. Thus, compared to the $\beta' = 0$ configuration, between $0 < \beta' \le \beta'_{c_1}$, with

increasing β', states with $\Lambda_{n_1}^-(\beta')$ are energetically more favorable to be filled by produced pairs, while between $\beta'_{c_1} \le \beta' \le \sqrt{2n_1 - 1}$, they still are more favorable to be filled but become less so with increasing β'. These features are reflected in the profile $f_0(y,\beta')$ as readily observed from Fig. 1(a); at around[10] $y \approx 1$, we see that $f_0(y,\beta')$ takes larger values with increasing $\beta' \le \beta'_{c_1}$, with $\beta'_{c_1} \approx \sqrt{3/8}$ well approximated by that associated to the lowest energy level Λ_1^-, while for $\beta'_{c_1} \le \beta' \lesssim \beta'_{c_2}$, we have $f_0(y,\beta')$ decreasing with increasing β' but exceeding its value at $\beta' = 0$ at sufficiently large values of y. Our numerical estimates give $f_0(y = 1.5, \beta' = 0.86) \approx 0.1046$, $f_0(y = 1.5, \beta' = 0) \approx 0.1024$, and $f_0(y = 1.5, \beta' = 0.87) \approx 0.1006$, placing $\beta'_{c_2} \approx 0.86$ at $y = 1.5$ with $\beta'_{c_2} \lesssim 1$ for $y \to \infty$. For $\beta' > 1$, we have $\Lambda_1^-(\beta') > \Lambda_1^-(\beta' = 0)$, and any further increase in the value of β' results in a sharp decrease of the function $f_0(y,\beta')$ and, hence, the pair-production rates.

We may also define the function $F_0(y,\beta') \coloneqq \frac{f_0(y,\beta')}{f_0(y,0)}$, which is not only a good measure for the relative pair-production rates, but also allows us to further elaborate on the significance of the values $\beta'_{c_1} = \sqrt{3/8}$ and $\beta' = 1$. Inspecting the profiles of $F_0(y,\beta')$ in Fig. 1(b), we see that $F_0(y,\beta')$ exceeds the value 1 at $y \approx 1$ and becomes larger with increasing β' within the interval $0 < \beta' \lesssim \sqrt{3/8}$. For $\sqrt{3/8} \le \beta' < 1$, $F_0(y,\beta')$ is above the value 1 only for sufficiently large y and increases with β', approaching the value 1, while for $\beta' > 1$ it quickly decreases and converges to zero. In addition to these features, which are in complete accord with conclusions we have reached by inspecting the profile of $f_0(y,\beta')$, we further see that, at $\beta' = 1$, $F_0(y,\beta')$ approaches to the value $1/2$ at large y, with $F_0(y = 2, \beta' = 1) \approx 0.5020$. This means that, at the critical value $\beta' = 1$, the pair-production rate quickly converges to half of what was found for the purely Abelian case ($\beta' = 0$) in [16]. This profile of $F_0(y,\beta')$ at

---

[9]This limit is essentially independent of the value of β' and easily evaluated at $\beta' = 0$ and, therefore, holds the same at any value of β' by continuity. With $\beta' = 0$, starting from the first line in (2.14) and performing the sum over the index n_1 first, we have

$$
\begin{aligned}
\lim_{y \to 0} f_0(y,\beta') &= \lim_{y \to 0} \frac{12}{\pi} \sum_{n=1}^{\infty} \frac{(-1)^{n+1}}{n} \frac{y}{\sinh n\pi y} \\
&= \frac{12}{\pi^2} \sum_{n=1}^{\infty} \frac{(-1)^{n+1}}{n^2} = \frac{12}{\pi^2} \eta(2) = 1,
\end{aligned}
$$

using the value of the Dirichlet eta function $\eta(2) = \frac{\pi^2}{12}$.

[10]At sufficiently large values of y, the contribution of both the sums in (2.14) become sufficiently small, allowing us to distinguish the effects of the energies $\Lambda_{n_1}^-(\beta')$ of the available quantum states on the pair-production rates.
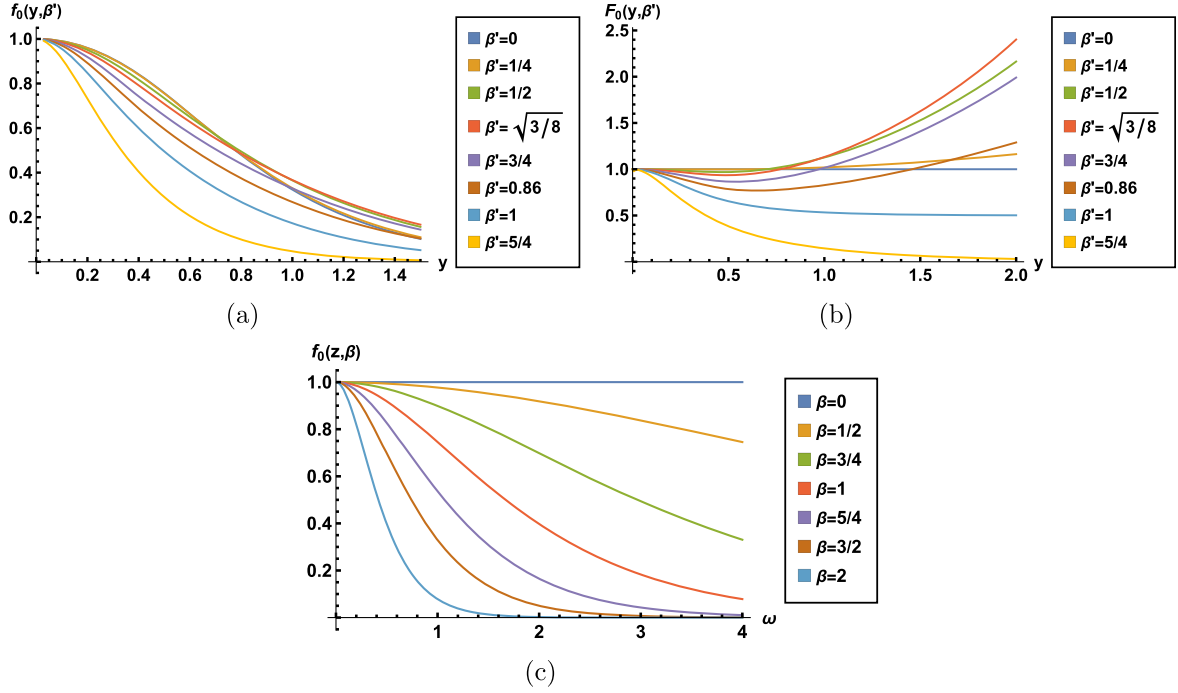
FIG. 1.   Profiles of $f_0(y, \beta')$ (a), $F_0(y, \beta')$ (b), and $f_0(z, \beta)$ (c).

$\beta' = 1$ can be predicted by comparing the energies and degeneracy of the lowest-lying quantum states. Indeed, we have[11] $\Lambda_0^+(\beta' = 0) = \Lambda_1^-(\beta' = 0) = B_1$ and $\Lambda_1^-(\beta' = 1) = B_1$; thus, we have double the number of states at this energy in the purely Abelian case leading to $F_0(y, \beta')$ converging to the value of $\frac{1}{2}$, which is corroborated from its profile given in Fig. 1(b).

The spectrum of $-D_{(1)}^2$ with purely non-Abelian magnetic field β is obtained from $\Lambda_{n_1}^\pm$ by taking the limit $B_1 \to 0$, $n_1 \to \infty$ such that $2B_1 n_1 \to k^2$ and $\Lambda_n^\pm \to = k^2 + 2\beta^2 \pm 2\beta k$, where $k = \sqrt{k_x^2 + k_y^2}$ and k_x, k_y are the eigenvalues of $\vec{p}$ in the transverse directions. This spectrum is also directly worked out from first principles in Appendix A for completeness. Computation of the Euclidean effective action Γ_E proceeds straightforwardly, and the short cut is that, in (2.14), $B_1 \sum_{n_1}$ gets replaced with the integral $\int k \, dk$, and this yields

$$\text{Re}(iS_{\text{eff}}) = -\int d^4x \, \frac{E^2}{96\pi} f_0(\pi/E, \beta), \qquad (2.15)$$

where

---

[11]Here, it is sufficient to focus on the lowest-lying energy eigenvalues, since they are the ones which are most easily filled by the produced pairs.

$$f_0(z, \beta) = \frac{12}{\pi^2} z \int k \, dk \Big(\ln(1 + e^{-z[(k+\beta)^2 + \beta^2 + m^2]}) \\ + \ln(1 + e^{-z[(k-\beta)^2 + \beta^2 + m^2]}) \Big). \qquad (2.16)$$

This is a decreasing function of β, as observed from Fig. 1(c), leading to a decrease in the pair-production rates with increasing β. In the limit $\beta \to 0$, we obtain twice the Schwinger result, since the dimension of the eigenstate space is trivially doubled due to the isospin degree of freedom.

III. PAIR-PRODUCTION RATES FOR SPINOR FIELDS FIELDS ON $\mathbb{R}^{3,1}$

We now proceed to consider the pair production for spin-$\frac{1}{2}$ particles on $\mathbb{R}^{3,1}$ under the influence of the same additional $SU(2) \times U(1)$ magnetic field. For this purpose, we again consider the Wick-rotated configuration with the magnetic fields F_{12} and F_{34} on $\mathbb{R}^2 \times \mathbb{R}^2 \equiv \mathbb{R}^4$. To our knowledge, the spectrum of the Dirac operator in such a background gauge field has not been considered in the literature before. Therefore, we proceed to handle this task first. We may note that the solution of this problem is interesting in its own right, as it leads to zero modes in a manner similar to the spectrum of the Dirac operator exposed to a purely Abelian uniform magnetic field.

A. Spectrum of the gauged Dirac operator

We may launch the discussion by writing out the gauged Dirac operator on the first copy of $\mathbb{R}^2$. This is given as

$$\not{D}_{(1)} = \gamma_i D_i = \gamma_i(\partial^i - iA^i_{(1)}), \qquad (3.1)$$

where γ_i are the 2×2 span the Clifford algebra on $\mathbb{R}^2$. We take them as $\gamma_1 = \tau_1$ and $\gamma_2 = \tau_2$, where τ_1 and τ_2 are the 2×2 Pauli matrices. The gauge field $A^i_{(1)}$ is as given already in (2.1). After some straightforward algebra which is relegated to Appendix B, we may write the operator $-\not{D}^2_{(1)}$ as

$$-\not{D}^2_{(1)} = 2B_1 \begin{pmatrix} a^\dagger a & \sqrt{2}\beta' a^\dagger & 0 & 0 \\ \sqrt{2}\beta' a & a^\dagger a + 2\beta'^2 & 0 & 0 \\ 0 & 0 & aa^\dagger + 2\beta'^2 & \sqrt{2}\beta' a^\dagger \\ 0 & 0 & \sqrt{2}\beta' a & aa^\dagger \end{pmatrix}, \qquad (3.2)$$

where a and $a^\dagger$ are the usual annihilation and creation operators, respectively (see Appendix A). Clearly, $-\not{D}^2_{(1)}$ is acting on the Hilbert space $\mathcal{H} = \mathbb{C}^4 \otimes \mathcal{F}$, where the Fock space $\mathcal{F}$ is spanned by the eigenstates of the number operator $N = a^\dagger a$ as usual. Diagonalizing $-\not{D}^2_{(1)}$ in an appropriate subspace $\mathcal{H}_n \subset \mathcal{H}$ leads to the spectrum (see Appendix B)

$$\lambda^\pm_{n_1} = B_1(1 + 2n_1 + 2\beta'^2 \pm \sqrt{1 + 4\beta'^2(1 + 2n_1 + \beta'^2)}), \qquad (3.3)$$

where $n_1 = 0, 1, \ldots$. We may remark that the $\pm$ signs in the spectrum $\lambda^\pm_{n_1}$ are correlated neither with the spin nor with the isospin of the system. Eigenstates of $-\not{D}^2_{(1)}$ are simultaneous eigenstates of the spin but not those of the isopin, since $-\not{D}^2_{(1)}$ commutes with τ_3 (for that matter, with

all τ_i) but not with σ_3. Thus, each eigenvalue occurs twice (once for spin up and once for spin down), and the density of states is $2 \times \frac{B_1}{2\pi}$. Details leading to these facts are provided in Appendix B. In particular, we may note that the $n_1 = 0$ level with the lower sign gives the zero modes and $\lambda^+_{n_1}$ ($\lambda^-_{n_1}$) is a monotonically increasing (decreasing) function of β'. Thus, all the eigenvalues $\lambda^-_{n_1}$ tend to zero as $\beta' \to \infty$.

We may note that the spectrum of $-\not{D}^2_{(2)}$ on the second $\mathbb{R}^2$ copy is that of the Dirac-Landau problem and given by $2B_2(n_2 + 1)$ and $2B_2 n_2$, for $n_2 = 0, 1, \ldots$, for spin up and down, respectively. Thus, the spectrum of $-\not{D}^2 + m^2 = -(\not{D}^2_{(1)} + \not{D}^2_{(2)}) + m^2$ on $\mathbb{R}^2 \times \mathbb{R}^2 = \mathbb{R}^4$ is easily written as

$$\text{Spec}(-\not{D}^2 + m^2) = \begin{cases} \lambda^\pm_{n_1} + 2B_2(n_2 + 1) + m^2, \\ \lambda^\pm_{n_1} + 2B_2 n_2 + m^2, \end{cases} \qquad (3.4)$$

where $n_1, n_2 = 0, 1, \ldots$ and the density of states is $2 \times B_1 B_2/(2\pi)^2$ in each branch.

B. Pair-production rates

In the Euclidean signature, the one-loop effective action is given as

$$\begin{aligned} \Gamma_E &= -\text{Tr}\ln(\not{D} + m) \\ &= -\frac{1}{2}\text{Tr}\ln(\not{D}^\dagger + m)(\not{D} + m) \\ &= -\frac{1}{2}\text{Tr}\ln(-\not{D}^2 + m^2). \end{aligned} \qquad (3.5)$$

Separating out the zero mode contribution explicitly and performing the summation over the index n_2, we get

$$\Gamma_E = \frac{B_1 B_2}{4\pi^2} \int d^4x \lim_{\epsilon \to 0} \frac{ds}{s} \coth sB_2 \left[\sum_{n_1=0}^\infty e^{-s\left(1+2n_1+2\beta'^2+\sqrt{1+4\beta'^2(1+2n_1+\beta'^2)}+m^2\right)} + \sum_{n_1=1}^\infty e^{-s\left(1+2n_1+2\beta'^2-\sqrt{1+4\beta'^2(1+2n_1+\beta'^2)}+m^2\right)} + e^{-sm^2} \right]. \qquad (3.6)$$

Equation (3.6) includes an overall of factor of 2, since each of the eigenvalues $\lambda^\pm_{n_1}$ occurs with multiplicity 2. Performing the integral over s, evaluating the sum due to the ensuing residue integration, and Wick rotating the Γ_E to Minkowski time allows us to write $\text{Re}(iS_{\text{eff}})$ as

$$\begin{aligned} \text{Re}(iS_{\text{eff}}) = -\int d^4x \frac{E^2}{2\pi^2} y \Bigg[&\ln(1 - e^{-\pi m^2/E}) + \sum_{n_1=0} \ln\left(1 - e^{-\pi m^2/E - y\pi(1+2n_1+2\beta'^2+\sqrt{1+4\beta'^2(1+2n_1+\beta'^2)})}\right) \\ &+ \sum_{n_1=1} \ln\left(1 - e^{-\pi m^2/E - y\pi(1+2n_1+2\beta'^2-\sqrt{1+4\beta'^2(1+2n_1+\beta'^2)})}\right) \Bigg], \end{aligned} \qquad (3.7)$$

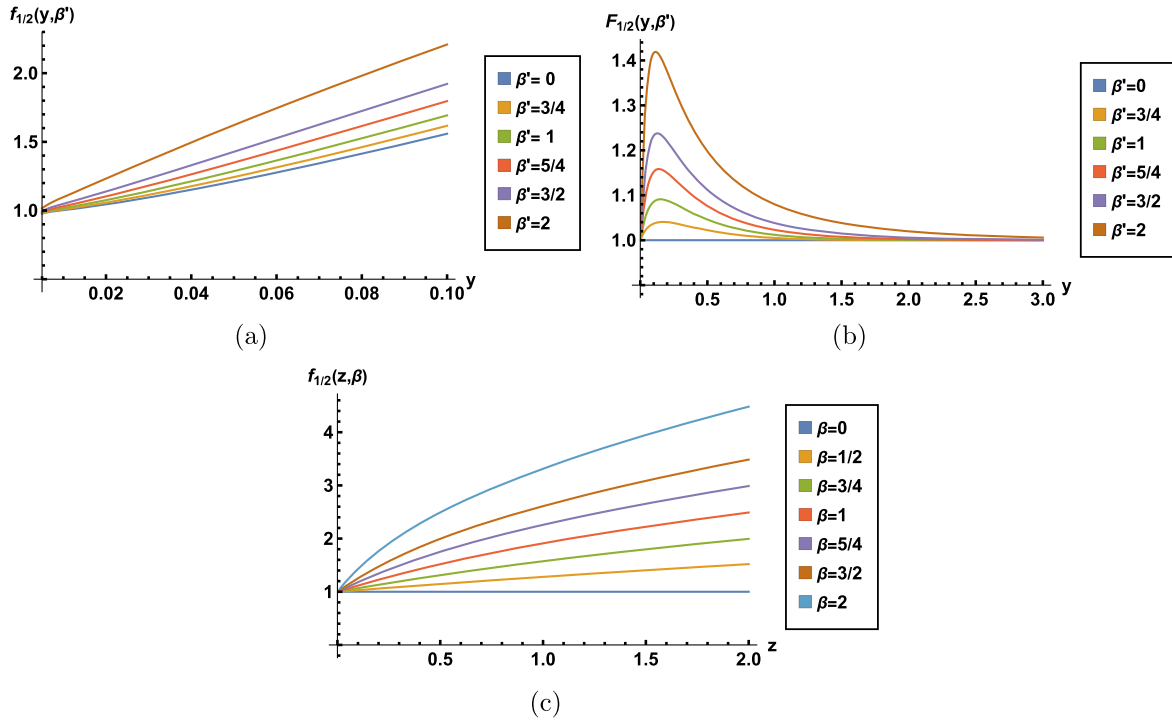where, we have, once again, used $y \equiv B_1/E$. We may write our final result as

FIG. 2.   Profiles of $f_{1/2}(y,\beta')$ (a), $F_{1/2}(y,\beta')$ (b), and $f_{1/2}(z,\beta)$ (c).

$$\mathrm{Re}(iS_{\mathrm{eff}}) = -\int d^4x \frac{E^2}{24\pi} f_{1/2}(y,\beta'), \tag{3.8}$$

where

$$f_{1/2}(y,\beta') = -\frac{6y}{\pi}\left[\ln(1-e^{-\pi m^2/E}) + \sum_{n_1=0}\ln\left(1-e^{-\pi m^2/E-y\pi(1+2n_1+2\beta'^2+\sqrt{1+4\beta'^2(1+2n_1+\beta'^2)})}\right)\right.$$

$$\left. + \sum_{n_1=1}\ln\left(1-e^{-\pi m^2/E-y\pi(1+2n_1+2\beta'^2-\sqrt{1+4\beta'^2(1+2n_1+\beta'^2)})}\right)\right]. \tag{3.9}$$

We may note that the first term in this expression is the contribution of the zero modes, which will make $f_{1/2}(y,\beta')$ diverge to infinity unless it is regulated. The mass term is kept as an infrared cutoff to avoid this divergent behavior. In the absence of the non-Abelian field, i.e., $\beta' = 0$, we already know that [16] $f_{1/2}(y,\beta') \to 1$ as $y \to 0$ and it increases with y. In the present case, since the degeneracy of the zero modes still increases with increasing values of B_1 (hence, increasing y), we expect an increase in the pair-production rates as y becomes larger, as there is no energy cost for the produced pairs to fill these zero energy states. The function $f_{1/2}(y,\beta')$ is rather sensitive to the choice of the infrared cutoff, and its profile is given Fig. 2(a), where we have picked $\frac{m^2\pi}{E} = 2 \times 10^{-2}$ and evaluated the sums up to $n_1 = 125$. Figure 2(a) clearly depicts these expectations, and we further observe that the function $f_{1/2}(y,\beta')$ and,

hence, the pair production goes up as we raise the value of β' at any fixed value of y. To better understand this feature, we note from (3.9) that, at any given value of y, the argument of the first sum tends to $\approx \ln 1 \to 0$, since $\lambda_{n_1}^+$ in the exponential is monotonically increasing with β', while the argument of the second sum tends to $\ln(1-e^{-\pi m^2/E})$, since $\lambda_{n_1}^-$ in the exponential is monotonically decreasing with β' starting with a maximum value of $2B_1 n_1$ at $\beta' = 0$. Thus, as β' becomes larger, all the terms in the second sum tend to contribute almost the same as with that of the zero modes, resulting in a sharp increase in the pair-production rates. Let us note in passing that the hierarchy in the plots with respect to β' in Fig. 2(a) is preserved at other physically sensible values of the cutoff $\frac{m^2\pi}{E}$. A good measure for the relative production rate is provided by the function $F_{1/2}(y,\beta') = \frac{f_{1/2}(y,\beta')}{f_{1/2}(y,0)}$, which is essentially

independent of the infrared cutoff,[12] and it is plotted in Fig. 2(b) at several values of β'. We immediately see the quickly formed peaks in the profile of this function at low values of y and, hence, the sharp increase in the pair-production rates compared to the purely Abelian case with $\beta' = 0$ as we keep on increasing β'. As y increases further, only the zero mode term $\ln(1 - e^{-\pi m^2/E})$ contributes significantly to both the numerator and denominator of $F_{1/2}(y, \beta')$, and the pair-production rates tend back to its value at $\beta' = 0$.

The spectrum of $-\not{D}^2_{(1)}$ with purely non-Abelian magnetic field β is obtained from $\lambda^{\pm}_{n_1}$ by taking the limit $B_1 \to 0$, $n_1 \to \infty$ such that $2B_1 n_1 \to k^2$. This gives $\lambda^{\pm}_n \to k^2 + 2\beta^2 \pm 2\beta\sqrt{k^2 + \beta^2}$, where $k = \sqrt{k_x^2 + k_y^2}$ as already defined in the previous section. For completeness, we provide a complete derivation of this spectrum from first principles in Appendix B. Absorbing the zero mode term in (3.7) back into the last sum in that expression and subsequently replacing $B_1 \sum_{n_1}$ with the integral $\int k\,dk$, we obtain

$$\text{Re}(iS_{\text{eff}}) = -\int d^4x \frac{E^2}{24\pi} f_{1/2}(\pi/E, \beta), \quad (3.10)$$

where

$$f_{1/2}(z, \beta) = -\frac{6}{\pi^2} z \int k\,dk \Big(\ln\big(1 - e^{-z[(k^2 + 2\beta^2 + 2\beta\sqrt{k^2 + \beta^2} + m^2)]}\big)$$
$$+ \ln\big(1 - e^{-z[k^2 + 2\beta^2 - 2\beta\sqrt{k^2 + \beta^2} + m^2]}\big) \Big). \quad (3.11)$$

This is an increasing function of β, leading to a significant increase in the pair-production rates as β becomes larger, as readily observed from the plots given in Fig. 2(c). In the $\beta \to 0$ limit, we recover twice the Schwinger result, due to equal contributions coming from the isospin up and isospin down degrees of freedom in this limit.

IV. PAIR-PRODUCTION RATES FOR SCALAR FIELDS FIELDS ON $S^2 \times \mathbb{R}^{1,1}$

In this section, we compute the pair-production rates for spin-0 and spin-$\frac{1}{2}$ particles subject to a radial $SU(2) \times U(1)$ magnetic field on the product manifold $S^2 \times \mathbb{R}^{1,1}$. To proceed, we follow a similar line of development as in the previous section and first evaluate the one-loop effective action on $S^2 \times \mathbb{R}^2$ with a radial $SU(2) \times U(1)$ magnetic field on S^2 and the usual uniform magnetic field on $\mathbb{R}^2$. The latter will then be Wick rotated to the uniform electric field as before.

---

[12]We have verified this numerically using *Mathematica*.

A. Spectrum of the gauged Laplacian on $S^2 \times \mathbb{R}^2$

To proceed, we need the spectrum of the gauged Laplacian

$$D^2 = \frac{\vec{\Lambda}^2}{a^2}, \qquad \vec{\Lambda} \equiv \vec{r} \times (\vec{p} - \vec{A}), \quad (4.1)$$

on S^2, where

$$\vec{A} = \vec{A}_{\text{Abelian}} + \alpha \frac{\vec{r} \times \vec{\sigma}}{a^2}, \quad (4.2)$$

a being the radius of S^2. Here, $\vec{A}_{\text{Abelian}}$ is the gauge potential for the Dirac monopole. The associated field strength is

$$B = \frac{N}{2a^2} + \left(2\left(\alpha - \frac{1}{2}\right)^2 - \frac{1}{2}\right)\frac{\vec{\sigma} \cdot \hat{r}}{a^2}, \quad (4.3)$$

where $N \in \mathbb{Z}$ stands for the Dirac monopole charge.

D^2 can be brought into the form

$$D^2 = \frac{1}{a^2}\left(\vec{J}^2 + \frac{1}{4} - \frac{N^2}{4} + 2\left(\alpha - \frac{1}{2}\right)^2 - \frac{1}{2} + 2\left(\alpha - \frac{1}{2}\right)\right.$$
$$\left. \times \left(\vec{J} \cdot \vec{\sigma} - \frac{1}{2} + \frac{N}{2}\vec{\sigma} \cdot \hat{r}\right) + \frac{N}{2}\vec{\sigma} \cdot \hat{r}\right), \quad (4.4)$$

where $\vec{J}$ is the total angular momentum, which is given as

$$\vec{J} = \vec{r} \times (\vec{p} - \vec{A}_{\text{Abelian}}) - \frac{N}{2}\hat{r} + \frac{\vec{\sigma}}{2},$$
$$= \vec{\Lambda}_{\text{Abelian}} - \frac{N}{2}\hat{r} + \frac{\vec{\sigma}}{2}. \quad (4.5)$$

$\vec{J}$ involves the contribution of the orbital angular momentum of the charged particle and that of the electromagnetic field generated by the particle-Dirac monopole pair as well as the contribution of the $SU(2)$ isospin. The spectrum of D^2 is already obtained in [28] and given by

$$\Lambda^{\pm}_{n_1}(\alpha) = \frac{1}{a^2}\left(n_1(N + n_1) + 2\left(\alpha - \frac{1}{2}\right)^2\right.$$
$$\left. - \frac{1}{2} \pm \sqrt{4\left(\alpha - \frac{1}{2}\right)^2(n_1 + N)n_1 + \frac{N^2}{4}}\right), \quad (4.6)$$

where we have $n_1 = 0, 1, 2, \dots$ for $\Lambda^+_{n_1}$ and $n_1 = 1, 2, \dots$ for $\Lambda^-_{n_1}$ and $N = 1, 2, \dots$. For convenience, we reproduce the calculation leading to this spectrum in Appendix C and also provide the group theoretical details that lead us to the $(2n_1 + N)$-fold degeneracy at each level and branch. Let us also note that $\Lambda^{\pm}_{n_1}(\alpha) = \Lambda^{\pm}_{n_1}(1 - \alpha)$, which is a consequence of the fact that B in (4.3) is symmetric under the

interchange $\alpha \leftrightarrow 1 - \alpha$. The spectrum of $D_{S^2}^2 + D_{\mathbb{R}^2}^2 + m^2$ on $S^2 \times \mathbb{R}^2$ is given as

$$\text{Spec}(D_{S^2}^2 + D_{\mathbb{R}^2}^2 + m^2) = \Lambda_{n_1}^{\pm}(\alpha) + B_2(2n_2 + 1) + m^2, \tag{4.7}$$

where n_1 is as given above and $n_2 = 0, 1, 2, \ldots$.

B. Pair-production rates

The Euclidean one-loop effective action takes the form

$$\Gamma_E = -\frac{1}{16\pi^2 a^2} \int d^2x \int d\Omega_2 \int \frac{ds}{s} \frac{B_2}{\sinh s B_2} \left[\sum_{n_1=0}^{\infty} (2n_1 + N) e^{-\frac{s}{a^2}\left[n_1(N+n_1)+2(\alpha-\frac{1}{2})^2-\frac{1}{2}+\sqrt{4(\alpha-\frac{1}{2})^2(n_1+N)n_1+\frac{N^2}{4}}\right]} \right.$$
$$\left. + \sum_{n_1=1}^{\infty} (2n_1 + N) e^{-\frac{s}{a^2}\left[n_1(N+n_1)+2(\alpha-\frac{1}{2})^2-\frac{1}{2}-\sqrt{4(\alpha-\frac{1}{2})^2(n_1+N)n_1+\frac{N^2}{4}}\right]} \right]. \tag{4.8}$$

Evaluating the integral over s and performing the Wick rotation $\mathbb{R}^2 \to \mathbb{R}^{1,1}$, $B_2 \to -iE$, we find

$$\text{Re}(iS_{\text{eff}}) = -\int d^2x \int d\Omega_2 \frac{E^2}{16\pi^3} \beta_0(\omega, \alpha, N), \tag{4.9}$$

where $\beta_0(\omega, \alpha, N)$ is given as

$$\beta_0(\omega, \alpha, N) = \omega \left[\sum_{n_1=0}^{\infty} (2n_1 + N) \ln\left(1 + e^{-\omega[n_1(N+n_1)+2(\alpha-\frac{1}{2})^2-\frac{1}{2}+\sqrt{4(\alpha-\frac{1}{2})^2 n_1(n_1+N)+\frac{N^2}{4}}]}\right) \right.$$
$$\left. + \sum_{n_1=1}^{\infty} (2n_1 + N) \ln\left(1 + e^{-\omega[n_1(N+n_1)+2(\alpha-\frac{1}{2})^2-\frac{1}{2}-\sqrt{4(\alpha-\frac{1}{2})^2 n_1(n_1+N)+\frac{N^2}{4}}]}\right) \right]. \tag{4.10}$$

In the above, we have defined $\omega := \pi/Ea^2$. Let us note immediately that $\beta_0(\omega, \alpha, N) = \beta_0(\omega, 1 - \alpha, N)$, which is clearly a consequence of the same symmetry that we have already noted for the spectrum in (4.6).

In order to compare the pair-production rates on this geometry to that on $\mathbb{R}^{3,1}$, we first evaluate the limit $S^2 \to \mathbb{R}^2$. To compute this, we take $a \to \infty$ and also $N, \alpha \to \infty$, while keeping both $\frac{N}{2a^2}$ and $\frac{\alpha^2}{a^2}$ constant. Since the definition of ω already contains the term $1/a^2$, we can keep ωN (or similar combinations) as is. We find

$$\beta_0^{\text{flat}}(\omega, \alpha, N) = \omega N \left[\sum_{n_1=0}^{\infty} \ln\left(1 + e^{-\omega[n_1 N + 2\alpha^2 + \sqrt{4\alpha^2 N n_1 + \frac{N^2}{4}}]}\right) \right.$$
$$\left. + \sum_{n_1=1}^{\infty} \ln\left(1 + e^{-\omega[n_1 N + 2\alpha^2 - \sqrt{4\alpha^2 N n_1 + \frac{N^2}{4}}]}\right) \right]. \tag{4.11}$$

In what follows, for notational ease, we write $\Lambda_{n_1}^{\pm \text{flat}} := \frac{1}{a^2}(n_1 N + 2\alpha^2 \pm \sqrt{4\alpha^2 N n_1 + N^2/4})$. We observe that the

latter identifies with (2.5) and $\beta_0^{\text{flat}}(\omega) \to \frac{\pi^2}{6} f_0(y, \beta')$ once we set $B_1 = \frac{N}{2a^2}$ and $\beta^2 = \frac{\alpha^2}{a^2}$ with $\beta'^2 = \frac{\beta^2}{B_1}$.

The ratio $\gamma_0(\omega, \alpha, N) \equiv \frac{\beta_0(\omega, \alpha, N)}{\beta_0^{\text{flat}}(\omega, \alpha, N)}$ is useful to compare the pair-production rates on $S^2 \times \mathbb{R}^{1,1}$ to that on $\mathbb{R}^{3,1}$.[13] We first inspect the profile of $\gamma_0(\omega, \alpha, N)$ from Figs. 3(a)–3(c) as we vary ω at $\alpha = 1/2, 1, 2$ at several N values. To elaborate on the physical meaning of the profiles of $\gamma_0(\omega, \alpha, N)$ and, hence, the relative pair-production rates, we essentially need to consider the hierarchy of only the lowest-lying energy levels for the spherical and flat geometries, which are Λ_0^+, Λ_1^- and $\Lambda_0^{+\text{flat}}$, $\Lambda_1^{-\text{flat}}$, respectively. In addition, we observe that the ratio of degeneracies of the curved to flat case goes as $\frac{N+2n_1}{N} = 1 + \frac{2n_1}{N}$, which may be understood as being due to the contribution of the curvature to the density of states,

---

[13]Let us note that $\gamma_0(\omega, \alpha, N) \neq \gamma_0(\omega, 1 - \alpha, N)$, since the denominator of $\gamma_0(\omega, \alpha, N)$ is not symmetric under $\alpha \leftrightarrow 1 - \alpha$. In particular, we may examine the relative pair-production rates for $\alpha < 0$, using only $\alpha > 1$ by forming the ratio $\tilde{\gamma}_0(\omega, \alpha, N) := \frac{\beta_0(\omega, 1-\alpha, N)}{\beta_0^{\text{flat}}(\omega, \alpha, N)}$.
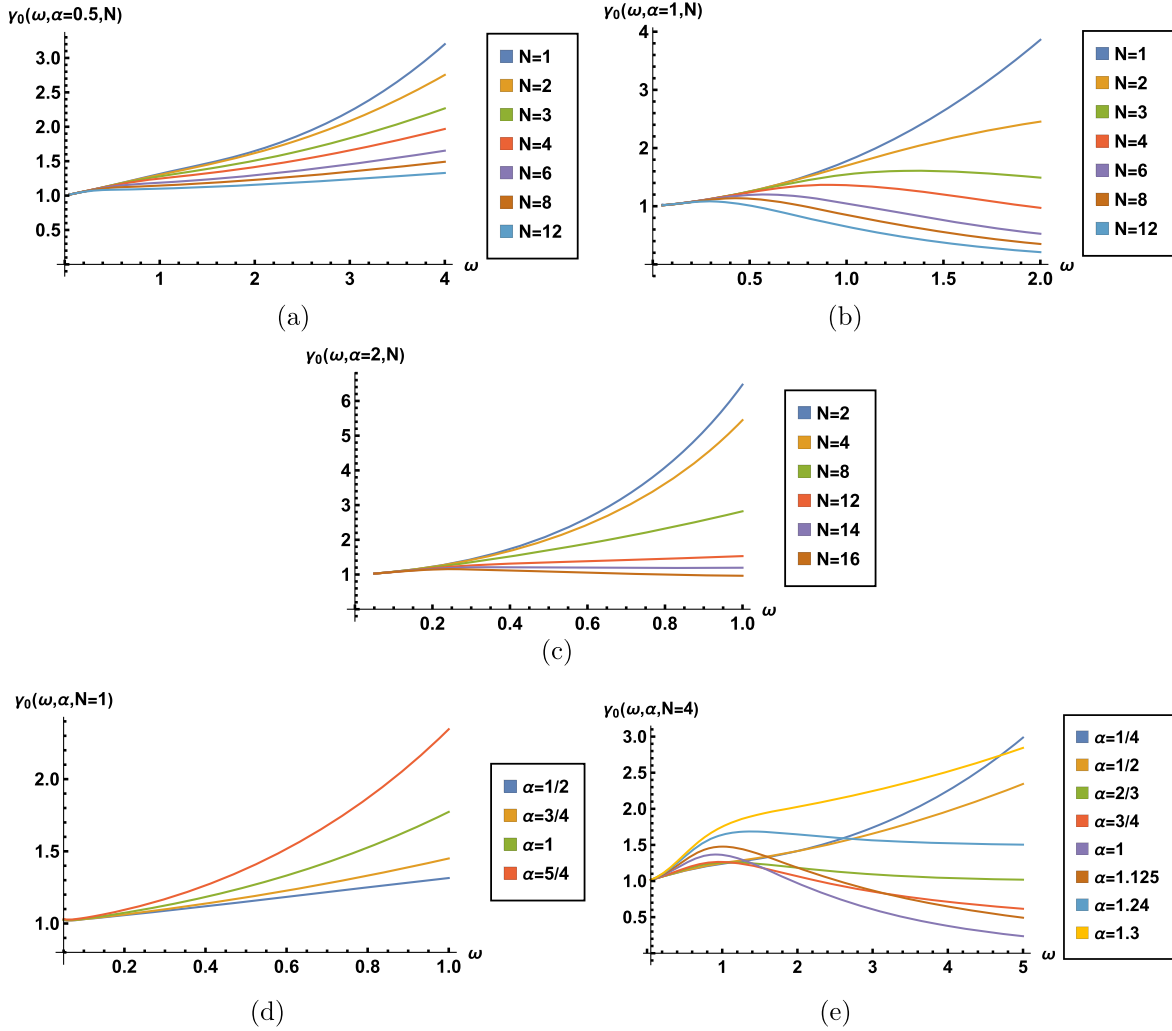
FIG. 3. RPP $\gamma_0(\omega, \alpha, N)$ as a function of ω.

which is $\frac{B_1}{2\pi} + \frac{2n_1}{4\pi a^2}$ as opposed to only $\frac{B_1}{2\pi}$ for the flat case [16], indicating improved availability of quantum states at any energy level except at $n_1 = 0$. Under the circumstances, that will be described shortly, the contribution of the second term in $\beta_0(\omega, \alpha, N)$ becomes important, $\gamma_0(\omega, \alpha, N)$ includes the

factor $1 + \frac{2}{N}$, whose enhancing effect tends to decrease with increasing N. These features completely govern the behavior of $\gamma_0(\omega, \alpha, N)$, with $\gamma_0(\omega, \alpha, N) > 1$ indicating relatively higher and $\gamma_0(\omega, \alpha, N) < 1$ lower pair-production amplitudes.
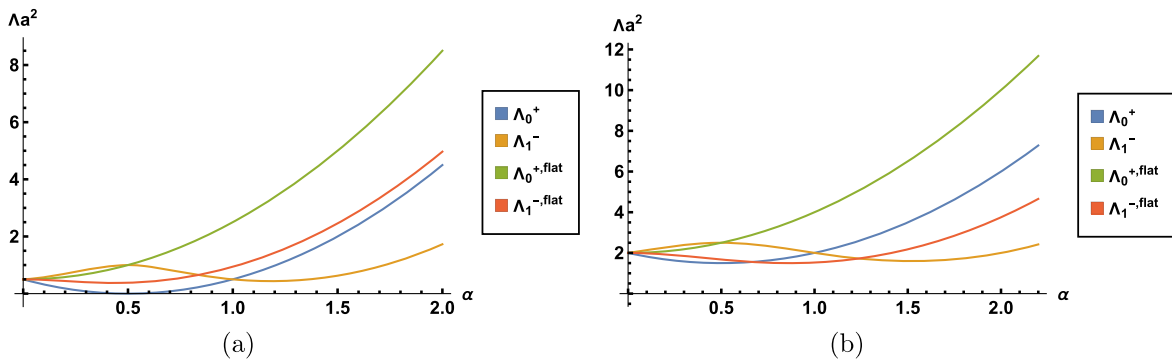

FIG. 4. Λ_0^+, Λ_1^-, $\Lambda_0^{+\,\text{flat}}$, and $\Lambda_1^{-\,\text{flat}}$ as a function of α, $N = 1$ (a), $N = 4$ (b).

We note that $\Lambda_0^+ < \Lambda_0^{+\text{flat}}$ (in fact, $\Lambda_{n_1}^+ < \Lambda_{n_1}^{+\text{flat}}$ for all $n_1 = 0, 1, 2, \ldots$) for all values of α, and Λ_0^+ and Λ_1^- intersect at $\alpha = 0$ and $\alpha = 1$ with $\Lambda_0^+ < \Lambda_1^-$ for $0 < \alpha < 1$ and $\Lambda_0^+ > \Lambda_1^-$ for $\alpha > 0$. Furthermore, we have Λ_0^+ intersecting $\Lambda_1^{-\text{flat}}$ at $\alpha_c^{(1)} = \frac{1}{2}\frac{N}{N-1}$ for $N \geq 2$, with $\Lambda_0^+ < \Lambda_1^{-\text{flat}}$ for $\alpha < \alpha_c^{(1)}$ and $\Lambda_0^+ > \Lambda_1^{-\text{flat}}$ for $\alpha > \alpha_c^{(1)}$, while for $N = 1$, $\alpha_c^{(1)} = 0$, since $\Lambda_0^+ = \frac{1}{2} = \Lambda_1^{-\text{flat}}$ at $\alpha = 0$ and Λ_0^+ remains always less than $\Lambda_1^{-\text{flat}}$ for $\alpha > 0$. Finally, Λ_1^- and $\Lambda_1^{-\text{flat}}$ intersect at $\alpha = 0$ and at $\alpha = \alpha_c^{(2)} > 1$, with $\Lambda_1^- > \Lambda_1^{-\text{flat}}$ for $\alpha < \alpha_c^{(2)}$ and $\Lambda_1^- < \Lambda_1^{-\text{flat}}$ for $\alpha > \alpha_c^{(2)}$, and where $\alpha_c^{(2)}$ is determined by the unique solution of $\frac{1}{N} = \frac{1}{16}\frac{1}{(\alpha-\frac{1}{2})^2} + \frac{1}{8}\frac{1}{(\alpha-\frac{1}{2})\alpha}$ for $\alpha \geq 1$ at a given value of $N = 2, 3 \ldots$, except at $N = 1$, for which $\alpha_c^{(2)} = 0.836$. At $N = 2$, we have $\alpha_c^{(2)} = 1$, and it gradually increases from this value with increasing N. For instance, $\alpha_c^{(2)} = 1.24$ at $N = 4$. We also note that, at $N = 2$, $\alpha_c^{(1)} = \alpha_c^{(2)} = 1$. Plots of these energy eigenvalues as a function of α at $N = 1$ and $N = 4$ are provided in Figs. 4(a) and 4(b) and clearly illustrate all the features which we have explained above. Putting these facts together, for $0 < \alpha < \alpha_c^{(1)}$, we have Λ_0^+ as the lowest-energy eigenvalue, so these states are energetically favored to be filled by the produced pairs in comparison with Λ_1^- as well as $\Lambda_0^{+\text{flat}}$ and $\Lambda_1^{-\text{flat}}$, and we, therefore, see from Figs. 3(a)–3(c) that $\gamma_0(\omega, \alpha, N)$ increases above its starting value 1, and, hence, we conclude that there is an increase in the relative pair-production probabilities. As the Dirac monopole charge N is increased, Λ_0^+ (as well as Λ_1^-, $\Lambda_0^{+\text{flat}}$, and $\Lambda_1^{-\text{flat}}$) also increases, and, therefore, the rate of increase in $\gamma_0(\omega, \alpha, N)$ slows down and it gradually tends to 1 as $N \to \infty$, indicating that the pair-production rates tend to converge toward what is found for the flat case. For $\alpha_c^{(1)} < \alpha < \alpha_c^{(2)}$, we have $\Lambda_1^{-\text{flat}}$ as the lowest among these four energies, and we eventually see that $\gamma_0(\omega, \alpha, N)$ goes below the value 1 (in fact, tends to zero at large ω) as expected. Nevertheless, within a narrow range of values of ω, approximately $0 < \omega \lesssim 1$, we also observe that $\gamma_0(\omega, \alpha, N) \geq 1$. The latter can be explained being due to approximately equal contributions from Λ_0^+ and Λ_1^- to the numerator beating those of $\Lambda_0^{+\text{flat}}$ and $\Lambda_1^{-\text{flat}}$ to the denominator.[14] Finally, for $\alpha > \alpha_c^{(2)}$, we have Λ_1^- become the lowest among these four energies leading to

$\gamma_0(\omega, \alpha, N) > 1$ and a significant increase in the relative pair-production amplitudes. We may note that, at $\alpha = \alpha_c^{(2)}$, $\gamma_0(\omega, \alpha, N)$ converges to the ratio of the degeneracies $1 + \frac{2}{N}$, except at $N = 1$. In the latter case, two facts—Λ_0^+ always remaining less than $\Lambda_1^{-\text{flat}}$ and $\Lambda_0^{+\text{flat}}$ being almost always the largest among the lowest-lying energies—are sufficient to ensure that $\gamma_0(\omega, \alpha, N = 1) > 1$ with a positive rate of change with increasing α. We may illustrate all of these conclusions by inspecting the profile of $\gamma_0(\omega, \alpha, N)$ at a fixed value of N and several distinct values of α. In Figs. 3(d) and 3(e), we give the plots of $\gamma_0(\omega, \alpha, N)$ at $N = 1$ and $N = 4$, for which $(\alpha_c^{(1)}, \alpha_c^{(2)}) = (0, 0.836)$ and $(\alpha_c^{(1)}, \alpha_c^{(2)}) = (1, 1.24)$, respectively. We see that, for $\omega \gtrsim 1$, $\gamma_0(\omega, \alpha, N = 4)$ is above the value 1 for all $0 < \alpha < \frac{2}{3}$ albeit decreasing with increasing α, and it goes below 1 for $\frac{2}{3} < \alpha < 1.24$.[15] At $\alpha = 1.24$, $\gamma_0(\omega, \alpha, N = 4) \to \frac{3}{2}$ for large ω, while it increases for $\alpha > 1.24$.

We may also compare the pair-production rates with and without the non-Abelian magnetic fields. For this purpose, we define $R_0(\omega, \alpha, N) \equiv \frac{\beta_0(\omega, \alpha, N)}{\beta_0(\omega, 0, N)}$. Plots of $R_0(\omega, \alpha, N)$ for $N = 1$ and $N = 4$ are provided in Figs. 5(a)–5(d), respectively. To explain the physics underneath, we first note that, in units of $\frac{1}{a^2}$, $\Lambda_{n_1}^\pm(\alpha = 0) = \Lambda_{n_1}^\pm(\alpha = 1)$ and $\Lambda_0^+(\alpha = 0, 1) = \frac{N}{2} = \Lambda_1^-(\alpha = 0, 1)$. We also have $\Lambda_0^+ \leq \frac{N}{2}$, $\Lambda_1^- \geq \frac{N}{2}$ for $0 \leq \alpha \leq 1$. At $\alpha = \frac{1}{2}$, Λ_0^+ has a global minimum (taking the value $\frac{N-1}{2}$) and Λ_1^- has a local maximum (taking the value $\frac{N+1}{2}$). For $\alpha > 1$, we have $\Lambda_0^+ > \frac{N}{2}$ and it increases monotonically with α, whereas Λ_1^- continues to decrease further, makes a minimum,[16] and monotonically increases from thereon attaining the value $\frac{N}{2}$ again at $\alpha_c^{(3)} := \frac{1}{2}(1 + \sqrt{2N+1})$. All of these features can be visibly recognized from Fig. 4(b). Keeping these facts in mind, we first note that $R_0(\omega, \alpha, N) = R_0(\omega, 1 - \alpha, N)$. Next, we observe that the large ω behavior of $R_0(\omega, \gamma, N)$ is described by

$$R_0(\omega, \alpha, N) \overset{\omega \to \infty}{\longrightarrow} \begin{cases} \infty & \alpha < \alpha_c^{(3)}, \alpha \neq 0, 1, \\ \frac{1}{2}\frac{N+2}{N+1} & \alpha = \alpha_c^{(3)}, \\ 0 & \alpha > \alpha_c^{(3)}, \end{cases} \tag{4.12}$$

---

[14]For instance, we may estimate $\gamma_0(\omega = 1/2, \alpha, N)$ at $N = 4$ and $\alpha = 1$. We have, in units of $\frac{1}{a^2}$, $\Lambda_0^+ = \Lambda_1^- = 2$, while $\Lambda_0^{+\text{flat}} = 4$, $\Lambda_1^{-\text{flat}} = 1.528$ and

$$\gamma_0(1/2, \alpha, N) \approx \frac{5}{4}\frac{2\ln(1 + e^{-1})}{\ln(1 + e^{-2}) + \ln(1 + e^{-0.85})} \approx 1.537,$$

while we have $\gamma_0(2, , \alpha, N) \approx \frac{5}{4}\frac{2\ln(1 + e^{-4})}{\ln(1 + e^{-8}) + \ln(1 + e^{-3.056})} \approx 0.979$.

[15]Even within this interval there is a subhierarchy: $\gamma_0(\omega, \alpha, N = 4)$ decreasing with increasing α up to $\alpha \approx 1$ and increasing for $\alpha > 1$ while it remains below the value 1. This is also understood as being due the counterplay among Λ_0^+, Λ_1^-, and $\Lambda_1^{-\text{flat}}$ all together.

[16]This is at $\alpha = \frac{1}{2} + \frac{1}{4}\sqrt{\frac{(N+2)(3N+2)}{N+1}}$, although it is not relevant for our purposes.
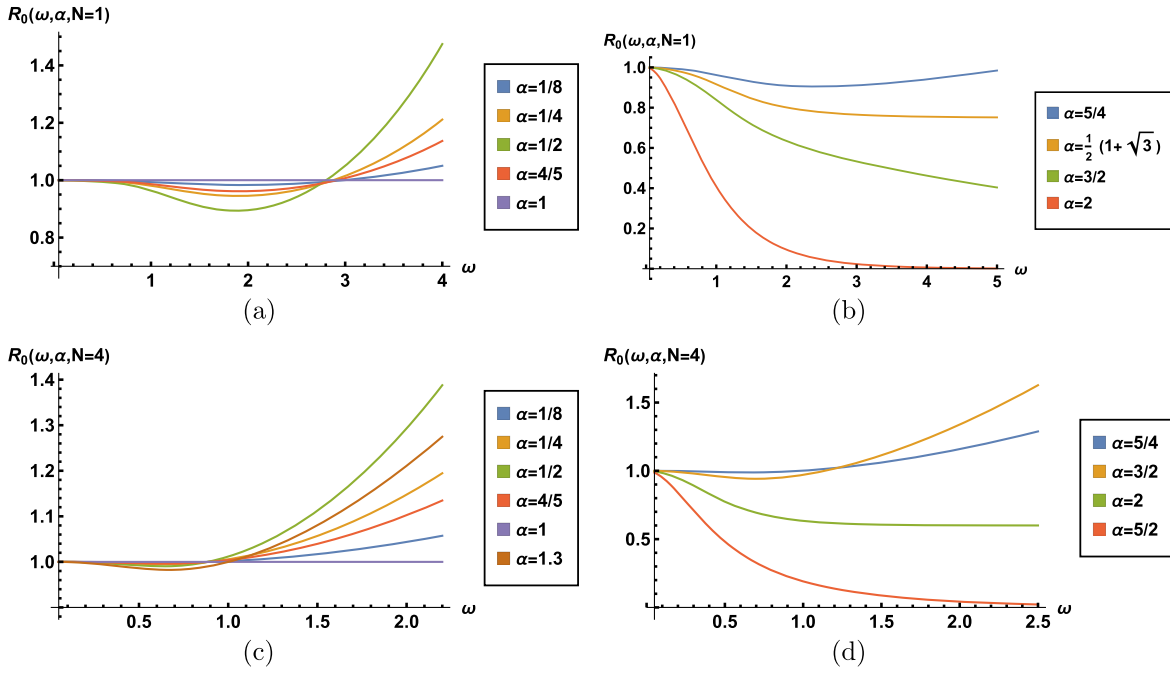
FIG. 5. $R_0(\omega, \alpha, N)$ as a function of ω.

where the limiting value $\frac{1}{2}\frac{N+2}{N+1}$ at $\alpha_c^{(3)}$ is readily seen to be simply the ratio of the degeneracy $N+2$ of the energy $\Lambda_1^-(\alpha_c^{(3)}) = \frac{N}{2}$ to the sum of the degeneracies N and $N+2$ of $\Lambda_0^+(\alpha = 0) = \frac{N}{2} = \Lambda_1^-(\alpha = 0)$, since the single former and the two latter energy levels yield an equivalent as well as the most dominant contribution $\ln(1 + e^{-\omega\frac{N}{2}})$ to the numerator and denominator of $R_0(\omega, \alpha, N)$, respectively. At large N, we have $R_0(\omega, \alpha_c^{(3)}, N) \rightarrow \frac{1}{2} + \frac{1}{2N}$; thus, it converges to $F_0(y, \beta' = 1) \approx \frac{1}{2}$ that we have found for the flat geometry while $\frac{\alpha_c^{(3)}}{a\sqrt{\frac{N}{2a^2}}} \approx 1 \rightarrow \beta'_c = 1$ as $a, N \rightarrow \infty$ (cf. Fig. 1(b) and the ensuing discussion). More generally, we have $R_0(\omega, \alpha, N) \rightarrow F_0(y, \beta')$ as $a, \alpha, N \rightarrow \infty$ with $B_1 = \frac{N}{2a^2}$, $\beta^2 = \frac{\alpha^2}{a^2}$, and $\beta'^2 = \frac{\beta^2}{B_1}$. We also see that, within $0 < \alpha < 1$, $R_0(\omega, \alpha, N) < 1$ around $\omega \approx \frac{2}{N}$ and increases above 1 afterward. This is a consequence of the counterplay between the contributions due to $\Lambda_0^+ \leq \frac{N}{2}$ and $\Lambda_1^- \geq \frac{N}{2}$ on one side and those of $\Lambda_0^+ = \frac{N}{2} = \Lambda_1^-$ at $\alpha = 0$ on the other. Since the degeneracies are N for Λ_0^+ and $N+2$ for Λ_1^-, the latter being slightly larger tilts the $R_0(\omega, \alpha, N)$ value below 1. Let us also that the rate of change of $R_0(\omega, \alpha, N)$ for both of these regimes (i.e., $R_0(\omega, \alpha, N) < 1$ and $R_0(\omega, \alpha, N) > 1$) is increasing for $0 < \alpha < \frac{1}{2}$ and decreasing for $\frac{1}{2} < \alpha < 1$ with a maximum at $\alpha = \frac{1}{2}$, while the rate of change of $R_0(\omega, \alpha, N)$ with respect to ω becomes slower for $R_0(\omega, \alpha, N) < 1$ and faster for $R_0(\omega, \alpha, N) > 1$ with increasing N. For $1 < \alpha < \alpha_c^{(3)}$, although $R_0(\omega, \alpha, N) \rightarrow \infty$ as $\omega \rightarrow \infty$, the interval over which $R_0(\omega, \alpha, N) < 1$ stretches longer with increasing α and eventually makes $R_0(\omega, \alpha, N)$ converge to $\frac{1}{2}\frac{N+2}{N+1}$ at $\alpha = \alpha_c^{(3)}$. Finally, for $\alpha > \alpha_c^{(3)}$, $R_0(\omega, \alpha, N)$ rapidly approaches to zero, since both Λ_0^+ and Λ_1^- are larger than the $\frac{N}{2}$ value they take at $\alpha = 0$.

For the case of vanishing Abelian monopole charge, the spectrum of D^2 on S^2 is given in (C16) in Appendix C. Using the latter, we find that

$$\mathrm{Re}(iS_{\mathrm{eff}}) = -\int d^2x \int d\Omega_2 \frac{E^2}{8\pi^3}\beta_0(\omega, \alpha), \tag{4.13}$$

where

$$\beta_0(\omega, \alpha) = \omega \sum_{l=1}^{\infty} l\left(\ln\left(1 + e^{-\omega[l^2 + 2(\alpha - \frac{1}{2})^2 - \frac{1}{2} + 2(\alpha - \frac{1}{2})l]}\right)\right.$$
$$\left. + \ln\left(1 + e^{-\omega[l^2 + 2(\alpha - \frac{1}{2})^2 - \frac{1}{2} - 2(\alpha - \frac{1}{2})l]}\right)\right). \tag{4.14}$$

We may note that, for $\alpha = 0$, the sum over the second term in (4.14) starts from $l = 0$, since the spectrum of $\Lambda_{l,N=0}^-$ starts with $l = 0$ as remarked in Appendix C. Nevertheless, the expression for $\beta_0(\omega, \alpha)$ holds the same in this case, too, due to the factor l in the summand which ensures that the $l = 0$ term of the sum yields a vanishing contribution. Let us note that we also have $\beta_0(\omega, \alpha) = \beta_0(\omega, 1 - \alpha)$, implying, in particular, that $\beta_0(\omega, 0) = \beta_0(\omega, 1)$. In the limit $a \rightarrow \infty$ keeping $\frac{\alpha}{a}$ fixed, we may write $\beta_0^{\mathrm{flat}}(\omega, \alpha) =$
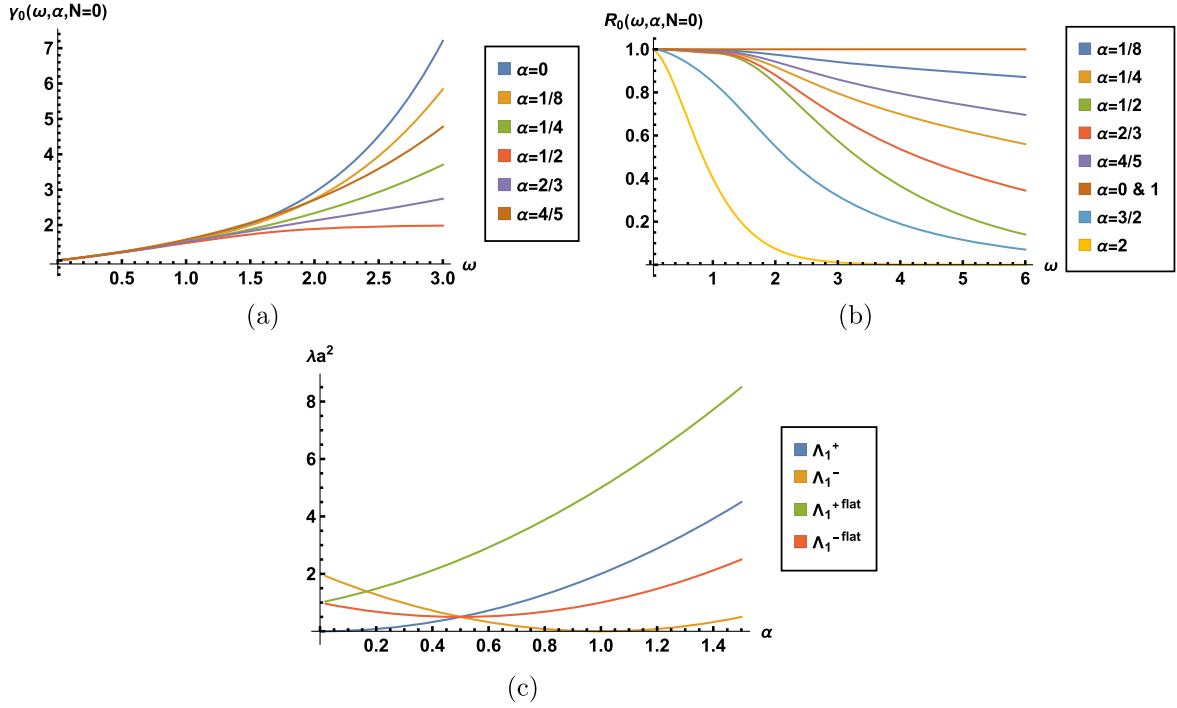
FIG. 6. $\gamma_0(\omega, \alpha)$ and $R_0(\omega, \alpha)$ at $N = 0$, Lowest lying energy eigenvalues as function of α (c).

$\omega \sum_{l=1}^{\infty} l(\ln(1 + e^{-\omega[(l+\alpha)^2 + \alpha^2]}) + \ln(1 + e^{-\omega[(l-\alpha)^2 + \alpha^2]}))$. In this limit, setting $\frac{l}{a} \to k$, $\frac{\alpha}{a} \to \beta$ and replacing $\frac{1}{a} \sum_l \frac{l}{a}$ with $\int k \, dk$, we find that $\beta_0^{\text{flat}}(\omega) \to \frac{\pi^2}{12} f_0(\frac{\pi}{E}, \beta, m = 0)$, where the last factor is given in (2.16). Below, we plot the profiles of $\gamma_0(\omega, \alpha) \equiv \frac{\beta_0(\omega, \alpha)}{\beta_0^{\text{flat}}(\omega, \alpha)}$ and $R_0(\omega, \alpha) \equiv \frac{\beta_0(\omega, \alpha)}{\beta_0(\omega, 0)}$. From Figs. 6(a) and 6(b), we see that the pair-production amplitude is larger compared to the flat case at all values of α and approaches to twice the latter as $\alpha \to \frac{1}{2}$ from either below or above. $\gamma_0(\omega, \alpha)$ decreases toward this value with increasing α for $0 < \alpha \leq \frac{1}{2}$ and with decreasing α for $\alpha > \frac{1}{2}$, as is readily inferred from the hierarchy among the lowest-lying energy states for the curved and the flat case. From Fig. 6(b), we see that $\Lambda_{l=1}^+(\alpha)$ is the lowest energy at $\alpha = 0$, and it mono-tonically increases with α passing through the value $\frac{1}{2}$ at $\alpha = \frac{1}{2}$ while both $\Lambda_{l=1}^-(\alpha)$ and $\Lambda_{l=1}^{-\text{flat}}(\alpha)$ decrease to their minimum value of $\frac{1}{2}$ at $\alpha = \frac{1}{2}$. Thus, we have $\Lambda_{l=1}^+(\frac{1}{2}) = \Lambda_{l=1}^-(\frac{1}{2}) = \Lambda_{l=1}^{-\text{flat}}(\frac{1}{2}) = \frac{1}{2}$, implying immediately that the limit $\gamma_0(\omega, \alpha = \frac{1}{2}) \to 2$ at large ω, since the numerator is dominated by the same eigenvalue with twice the multiplicity.

V. PAIR-PRODUCTION RATES FOR SPINOR FIELDS FIELDS ON $S^2 \times \mathbb{R}^{1,1}$

A. Spectrum of the gauged Dirac operator

In this section, we will calculate the pair-production rate for spinor fields on $S^2 \times \mathbb{R}^{1,1}$ under the influence of the same background fields introduced in the previous section. For this purpose, we need the spectrum of the square of the gauged Dirac operator $\not{D}^2 = \frac{1}{a^2}(\vec{\tau} \cdot \vec{\Lambda} + 1)^2$ on S^2, where τ_i are the usual Pauli matrices spanning the spin space. This is an interesting problem in its own right, which we fully solve in Appendix D. In terms of the total angular momentum $\vec{K} = \vec{L} + \frac{\vec{\sigma}}{2} + \frac{\vec{\tau}}{2}$, we have

$$a^2 \not{D}^2 = K^2 - \left(\frac{N^2}{4} - 2\left(\alpha - \frac{1}{2}\right)^2\right) + \chi, \quad (5.1)$$

where $\chi := 2(\alpha - \frac{1}{2})(\vec{K} \cdot \vec{\sigma} - \frac{1}{2}) + N\alpha \vec{\sigma} \cdot \hat{r} - 2\alpha(\alpha - \frac{1}{2})(\vec{\sigma} \cdot \hat{r})(\vec{\tau} \cdot \hat{r})$ and squares to the diagonal operator

$$\chi^2 = 4\left(\alpha - \frac{1}{2}\right)^2\left(K^2 + \frac{1}{4}\right) - \left(\left(\alpha - \frac{1}{2}\right)^2 - \frac{1}{4}\right)$$
$$\times \left(N^2 - 4\left(\alpha - \frac{1}{2}\right)^2\right), \quad (5.2)$$

in the $\vec{K}$ basis. Relegating the details of the calculations to Appendix D, the spectrum of $\not{D}_{S^2}^2 + \not{D}_{\mathbb{R}^2}^2$ on $S^2 \times \mathbb{R}^2$ is given in Table I, where

TABLE I. Spectrum of $\not{D}^2_{S^2} + \not{D}^2_{\mathbb{R}^2}$ and the corresponding density of states.

Spec($\not{D}^2_{S^2} + \not{D}^2_{\mathbb{R}^2} + m^2$)	Density of states
$\lambda_{n_1-1} + 2n_2 B_2$	$\frac{B_2}{2\pi} \frac{(2n_1+N-1)}{4\pi a^2}$
$\lambda^{\pm}_{n_1} + 2n_2 B_2$	$\frac{B_2}{2\pi} \frac{(2n_1+N+1)}{4\pi a^2}$
$\lambda_{n_1+1} + 2n_2 B_2$	$\frac{B_2}{2\pi} \frac{(2n_1+N+3)}{4\pi a^2}$
$\lambda_{n_1-1} + 2n_2 B_2 + 2$	$\frac{B_2}{2\pi} \frac{(2n_1+N-1)}{4\pi a^2}$
$\lambda^{\pm}_{n_1} + 2n_2 B_2 + 2$	$\frac{B_2}{2\pi} \frac{(2n_1+N+1)}{4\pi a^2}$
$\lambda_{n_1-1} + 2n_2 B_2 + 2$	$\frac{B_2}{2\pi} \frac{(2n_1+N+3)}{4\pi a^2}$

$$\lambda^{\pm}_{n_1}(\alpha) = \frac{1}{a^2}\left(\xi_{n_1} + \left(\alpha - \frac{1}{2}\right)^2 \pm \sqrt{4\left(\alpha - \frac{1}{2}\right)^2 \xi_{n_1} + \frac{N^2}{4}}\right),$$

(5.3)

$\xi_{n_1} = (n_1 + \frac{1}{2})^2 + N(n_1 + \frac{1}{2}) + ((\alpha - \frac{1}{2})^2 - \frac{1}{4})$. In the table, we have used the notation $\lambda_{n_1+1} := \lambda^-_{n_1+1}$, $\lambda_{n_1-1} := \lambda^+_{n_1-1}$, and we remark that, in the latter, for $n_1 = 0$ and $N \geq 2$,

$\sqrt{4(\alpha - \frac{1}{2})^2 \xi_{n_1-1} + N^2/4}$ is replaced with $\frac{N}{2} - 2(\alpha - \frac{1}{2})^2$ as explained in Appendix D. We have $n_1 = 0, 1, 2, ..., n_2 = 0, 1, 2, ...$ except for λ_{n_1-1} at $N = 1$ for which $n_1 = 1, 2, ...$. From detailed considerations given in Appendix D, we see that, for $N \geq 2$, the spectrum of $\not{D}^2_{S^2}$ has the zero modes $\lambda^-_0 = 0$ and $\lambda_{-1} = 0$ at $n_1 = 0$. However, for $N = 1$, we have from (D7c) that the set of eigenvalues λ_{n_1-1} starts with $n_1 = 1$, meaning that this branch does not include a zero mode, while the zero mode from the branch $\lambda^-_{n_1}$ is retained. Also note that the entire spectrum is symmetric under $\alpha \leftrightarrow 1 - \alpha$.

B. Pair-production rates

We first evaluate the effective action on $S^2 \times \mathbb{R}^2$ and then Wick rotate to $S^2 \times \mathbb{R}^{1,1}$. We have

$$\Gamma_E = \frac{1}{2}\int \frac{ds}{s} \text{Tr}[e^{-s(\not{D}^2+m^2)}].$$

(5.4)

Taking the integral over s and Wick rotating by letting $x_4 \to ix_0$ and $B_2 \to -iE$, the real part of iS_{eff} on $S^2 \times \mathbb{R}^{1,1}$ can be written (for $N \geq 2$) as

$$\text{Re}(iS_{\text{eff}}) = -\frac{1}{16\pi^2 a^2}\int d^2x \int d\Omega_2 \sum_{n=1}^{\infty} e^{-n\pi m^2/E} \frac{E}{n}\left\{\sum_{n_1=0}(2n_1+N-1)\left[e^{-n\pi(\xi_{n_1-1}+(\alpha-\frac{1}{2})^2+\sqrt{4(\alpha-\frac{1}{2})^2\xi_{n_1-1}+\frac{N^2}{4}}+m^2 a^2)/(Ea^2)}\right]\right.$$

$$+ \sum_{n_1=0}(2n_1+N+1)\left[e^{-n\pi(\xi_{n_1}+(\alpha-\frac{1}{2})^2+\sqrt{4(\alpha-\frac{1}{2})^2\xi_{n_1}+\frac{N^2}{4}}+m^2 a^2)/(Ea^2)}\right]$$

$$+ \sum_{n_1=0}(2n_1+N+1)\left[e^{-n\pi(\xi_{n_1}+(\alpha-\frac{1}{2})^2-\sqrt{4(\alpha-\frac{1}{2})^2\xi_{n_1}+\frac{N^2}{4}}+m^2 a^2)/(Ea^2)}\right]$$

$$\left.+ \sum_{n_1=0}(2n_1+N+3)\left[e^{-n\pi(\xi_{n_1+1}+(\alpha-\frac{1}{2})^2-\sqrt{4(\alpha-\frac{1}{2})^2\xi_{n_1+1}+\frac{N^2}{4}}+m^2 a^2)/(Ea^2)}\right]\right\}.$$

(5.5)

Using $\omega = \frac{\pi}{Ea^2}$, we can write $\text{Re}(iS_{\text{eff}})$ as

$$\text{Re}(iS_{\text{eff}}) = -\int d^2x \int d\Omega_2 \frac{E^2}{8\pi^3}\beta_{1/2}(\omega, \alpha, N),$$

(5.6)

where

$$\beta_{1/2}(\omega, \alpha, N) = -\frac{\omega}{2}\left\{2N\ln(1 - e^{-\omega m^2 a^2}) + \sum_{n_1=1}^{\infty}(2n_1+N-1)\ln(1 - e^{-\omega(\xi_{n_1-1}+(\alpha-\frac{1}{2})^2+\sqrt{4(\alpha-\frac{1}{2})^2\xi_{n_1-1}+\frac{N^2}{4}})+m^2 a^2})\right.$$

$$+ \sum_{n_1=0}^{\infty}(2n_1+N+1)\ln(1 - e^{-\omega(\xi_{n_1}+(\alpha-\frac{1}{2})^2+\sqrt{4(\alpha-\frac{1}{2})^2\xi_{n_1}+\frac{N^2}{4}})+m^2 a^2})$$

$$+ \sum_{n_1=1}^{\infty}(2n_1+N+1)\ln(1 - e^{-\omega(\xi_{n_1}+(\alpha-\frac{1}{2})^2-\sqrt{4(\alpha-\frac{1}{2})^2\xi_{n_1}+\frac{N^2}{4}})+m^2 a^2})$$

$$\left.+ \sum_{n_1=0}^{\infty}(2n_1+N+3)\ln(1 - e^{-\omega(\xi_{n_1+1}+(\alpha-\frac{1}{2})^2-\sqrt{4(\alpha-\frac{1}{2})^2\xi_{n_1+1}+\frac{N^2}{4}})+m^2 a^2})\right\}.$$

(5.7)

In (5.7), we have written the contribution of the zero modes explicitly. For $N = 1$, we have the first sum in (5.5) starting from $n_1 = 1$, and, hence, $\beta_{1/2}(\omega, \alpha, N)$ has the same form except that there is no factor of 2 in front of the first term in (5.7). We note that $\beta_{1/2}(\omega, \alpha, N) = \beta_{1/2}(\omega, 1 - \alpha, N)$.

We can calculate the form $\beta_{1/2}(\omega, \alpha, N)$ takes in the limit $S^2 \times \mathbb{R}^{1,1} \to \mathbb{R}^{3,1}$. We let $a \to \infty$, $N \to \infty$, and $\alpha \to \infty$ while keeping $N/2a^2$ and α^2/a^2 constant. Since ω

is proportional to $1/a^2$, this practically means we can keep $\omega\alpha^2$ and ωN as such, while the terms which vanish as $a \to \infty$ are dropped. We find, for $N \geq 2$, $\lambda_{n_1}^{\pm} \to \lambda_{n_1}^{\pm\text{flat}} =$

$$N(n_1 + \tfrac{1}{2}) + 2\alpha^2 + \pm\sqrt{4\alpha^2(N(n_1 + \tfrac{1}{2}) + \alpha^2) + \tfrac{N^2}{4}} \quad \text{and}$$

$\lambda_{n_1 \pm 1} \to \lambda_{n_1 \pm 1}^{\text{flat}}$ and, hence,

$$\beta_{1/2}^{\text{flat}}(\omega, \alpha, N) = -\frac{\omega N}{2}\left\{ 2\ln(1 - e^{-\omega m^2 a^2}) + \sum_{n_1=1}^{\infty} \ln(1 - e^{-\omega(N(n_1 - \frac{1}{2}) + 2\alpha^2 + \sqrt{4\alpha^2(N(n_1 - \frac{1}{2}) + \alpha^2) + \frac{N^2}{4}} + m^2 a^2)}) \right.$$

$$+ \sum_{n_1=0}^{\infty} \ln(1 - e^{-\omega(N(n_1 + \frac{1}{2}) + 2\alpha^2 + \sqrt{4\alpha^2(N(n_1 + \frac{1}{2}) + \alpha^2) + \frac{N^2}{4}} + m^2 a^2)})$$

$$+ \sum_{n_1=1}^{\infty} \ln(1 - e^{-\omega(N(n_1 + \frac{1}{2}) + 2\alpha^2 - \sqrt{4\alpha^2(N(n_1 + \frac{1}{2}) + \alpha^2) + \frac{N^2}{4}} + m^2 a^2)})$$

$$\left. + \sum_{n_1=0}^{\infty} \ln(1 - e^{-\omega(N(n_1 + \frac{3}{2}) + 2\alpha^2 - \sqrt{4\alpha^2(N(n_1 + \frac{3}{2}) + \alpha^2) + \frac{N^2}{4}} + m^2 a^2)}) \right\}. \tag{5.8}$$

Shifting the index of first sum in (5.8), it is seen to be equal to the second sum in (5.8); similarly shifting the index of the last sum to 1, it is seen to be equivalent to the third sum in (5.8). Thus, we obtain

$$\beta_{1/2}^{\text{flat}}(\omega, \alpha, N) = -\omega N\left\{ \ln(1 - e^{-\omega m^2 a^2}) + \sum_{n_1=0}^{\infty} \ln(1 - e^{-\omega(N(n_1 + \frac{1}{2}) + 2\alpha^2 + \sqrt{4\alpha^2(N(n_1 + \frac{1}{2}) + \alpha^2) + \frac{N^2}{4}} + m^2 a^2)}) \right.$$

$$\left. + \sum_{n_1=1}^{\infty} \ln(1 - e^{-\omega(N(n_1 + \frac{1}{2}) + 2\alpha^2 - \sqrt{4\alpha^2(N(n_1 + \frac{1}{2}) + \alpha^2) + \frac{N^2}{4}} + m^2 a^2)}) \right\}. \tag{5.9}$$

Using $B_1 = \frac{N}{2a^2}$ and $\beta = \frac{\alpha^2}{a^2}$, we find that $\beta_{1/2}^{\text{flat}}(\omega, \alpha, N) = \frac{\pi^2}{3}f_{1/2}(y, \beta')$ [cf. (3.9)]. We note that, for $N = 1$, there is no factor of 2 in front of the first term in the right-hand side of (5.8), and, consequently, there is factor of $\frac{1}{2}$ in front of the first term in the rhs of (5.9).

In order to compare the effects of curvature and the magnetic fields on the pair-production rates, we define the ratio $\gamma_{1/2}(\omega, \alpha, N) \coloneqq \frac{\beta_{1/2}(\omega, \alpha, N)}{\beta_{1/2}^{\text{flat}}(\omega, \alpha, N)}$. In Fig. 7, we plot the profile of $\gamma_{1/2}(\omega, \alpha, N)$ at both a fixed value of the non-Abelian charge α at different monopole strengths N as well as at several values of α at a fixed N. We observe that the pair-production rate remains less than that on the flat space at given values of N and α. This is mainly due to the n_1^2 dependence of the eigenvalues (which is due to the curvature effects) in the numerator causing it to be less than the denominator of $\gamma_{1/2}(\omega, \alpha, N)$. More concretely, the energies λ_{n_1+1} and $\lambda_{m_1-1}^+ = \lambda_{m_1-1}$ are larger than $\lambda_{n_1+1}^{-\text{flat}} = \lambda_{n_1+1}^{\text{flat}}$, where $n_1 = 0, 1, 2, \ldots$ and $m_1 = 1, 2, \ldots$, and, hence, the former are relatively harder to get filled by the produced pairs. An increase in α triggers a decrease

in $\gamma_{1/2}(\omega, \alpha, N)$, since $\lambda_{n_1+1}^{-\text{flat}}$ decreases with α and the associated flat levels become relatively easier to get filled compared to those in the curved background. These facts are readily observed from the plots given in Fig. 8. With increasing N, terms due to the zero modes become the dominant contribution, and they drive $\gamma_{1/2}(\omega, \alpha, N)$ back to the value 1 at large ω and, hence, the pair-production rate to that of the flat case. Our results are essentially independent of the infrared cutoff value for any physically reasonable choice of the latter. In our calculations, we have used $m^2 a^2 = \frac{1}{2}$.

It is also noteworthy to emphasize that the overall effect for $\alpha \neq 0$ is greater than that without the non-Abelian field (i.e., $\alpha = 0$). To see this, we can readily inspect the profiles of $R_{1/2}(\omega, N, \alpha) \equiv \frac{\beta_{1/2}(\omega, N, \alpha)}{\beta_{1/2}(\omega, N, 0)}$. Plots at $N = 1$, 2 at several values of α are given in Figs. 9(a)–9(d) and for $\alpha = 2$ at several values of N in Fig. 9(e). We see that there is an increase in the pair production for $\alpha \neq 0$ compared to $\alpha = 0$, while the rate of change in $R_{1/2}(\omega, N, \alpha)$ decreases as N assumes larger values [see Fig. 9(e)]. We also observe
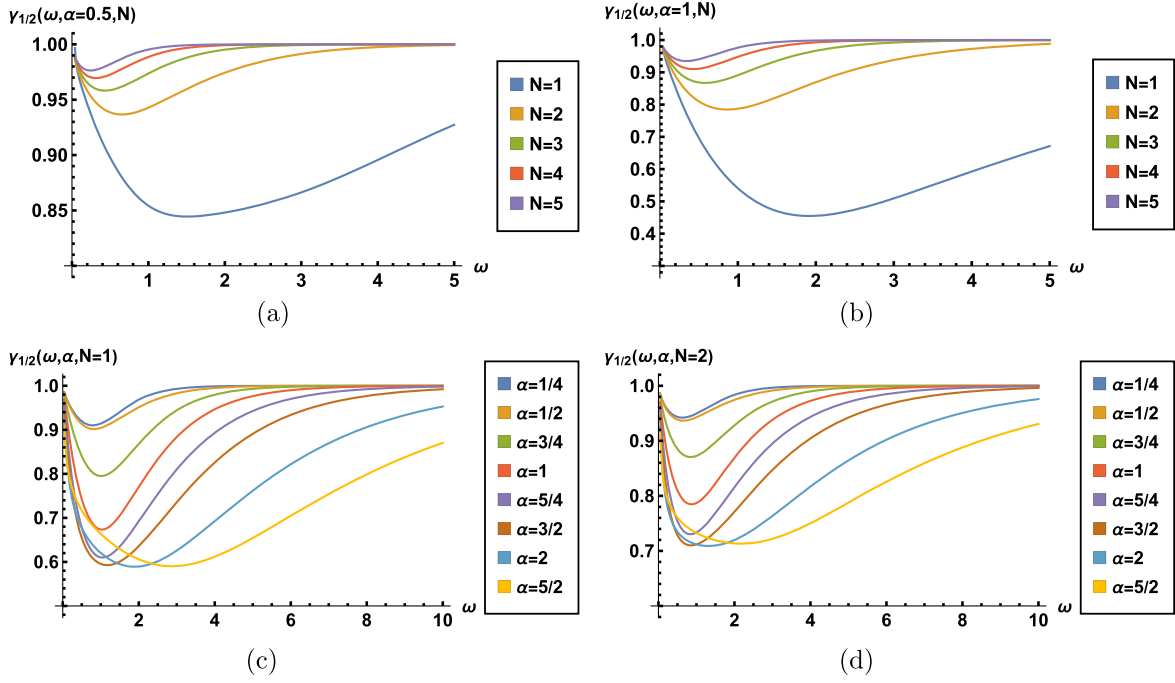
FIG. 7. $\gamma_{1/2}(\omega, \alpha, N)$ as a function of ω.

that, as ω becomes large, the pair-production rates converge back to what they are at $\alpha = 0$. The latter two results are due to the dominating effect of the zero modes at larger values of N and ω. For $\alpha > 1$, at fixed N, $R_{1/2}(\omega, N, \alpha)$ becomes larger with increasing α before it converges to 1 at large ω, while for $0 \leq \alpha < \frac{1}{2}$, we see that $R_{1/2}(\omega, N, \alpha)$ increases with α and decreases toward the value 1 in the interval $\frac{1}{2} < \alpha \leq 1$ and $R_{1/2}(\omega, N, \alpha = 1) = 1$. All of these features are readily explained by noting that, for $0 \leq \alpha \leq \frac{1}{2}$, $\lambda_{n_1}^+ < \lambda_{n_1}^+|_{\alpha=0} = \lambda_{n_1+1}|_{\alpha=0} = \lambda_{(n_1+1)-1}|_{\alpha=0} = (n_1 + 1)$ $(N + n_1 + 1)$, $n_1 = 0, 1, 2, \ldots$, with $\lambda_{n_1}^+$ becoming smaller with increasing α and reaching a local minimum at $\alpha = \frac{1}{2}$, while for $\frac{1}{2} \leq \alpha \leq 1$ the same inequality continues to hold with $\lambda_{n_1}^+$ increasing with α and becoming $(n_1 + 1)(N + n_1 + 1)$ at $\alpha = 1$. For $\alpha > 1$, we have $\lambda_{n_1+1} < (n_1 + 1)$ $(N + n_1 + 1)$ and $\lambda_{n_1}^+ > (n_1 + 1)(N + n_1 + 1)$, with the former being energetically more favorable to get filled and

hence leading to an increased amplitude for the pair production. Taking, $a, \alpha, N \to \infty$ with $B_1 = \frac{N}{2a^2}$, $\beta^2 = \frac{\alpha^2}{a^2}$ and $\beta'^2 = \frac{\beta^2}{B_1}$, we have $R_{1/2}(\omega, \alpha, N) \to F_{1/2}(y, \beta')$ as readily inferred from the definition of $R_{1/2}(\omega, N, \alpha)$.

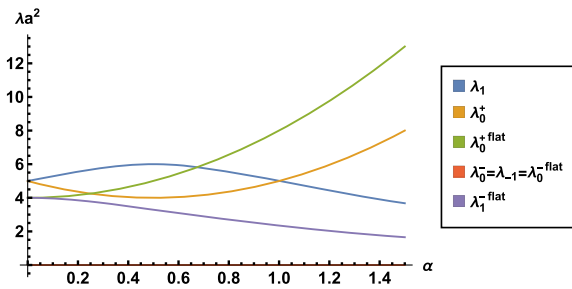For the case of vanishing abelian monopole charge the spectrum of $\not{D}_{S^2}^2$ is given in (D12). Using the latter, we find that
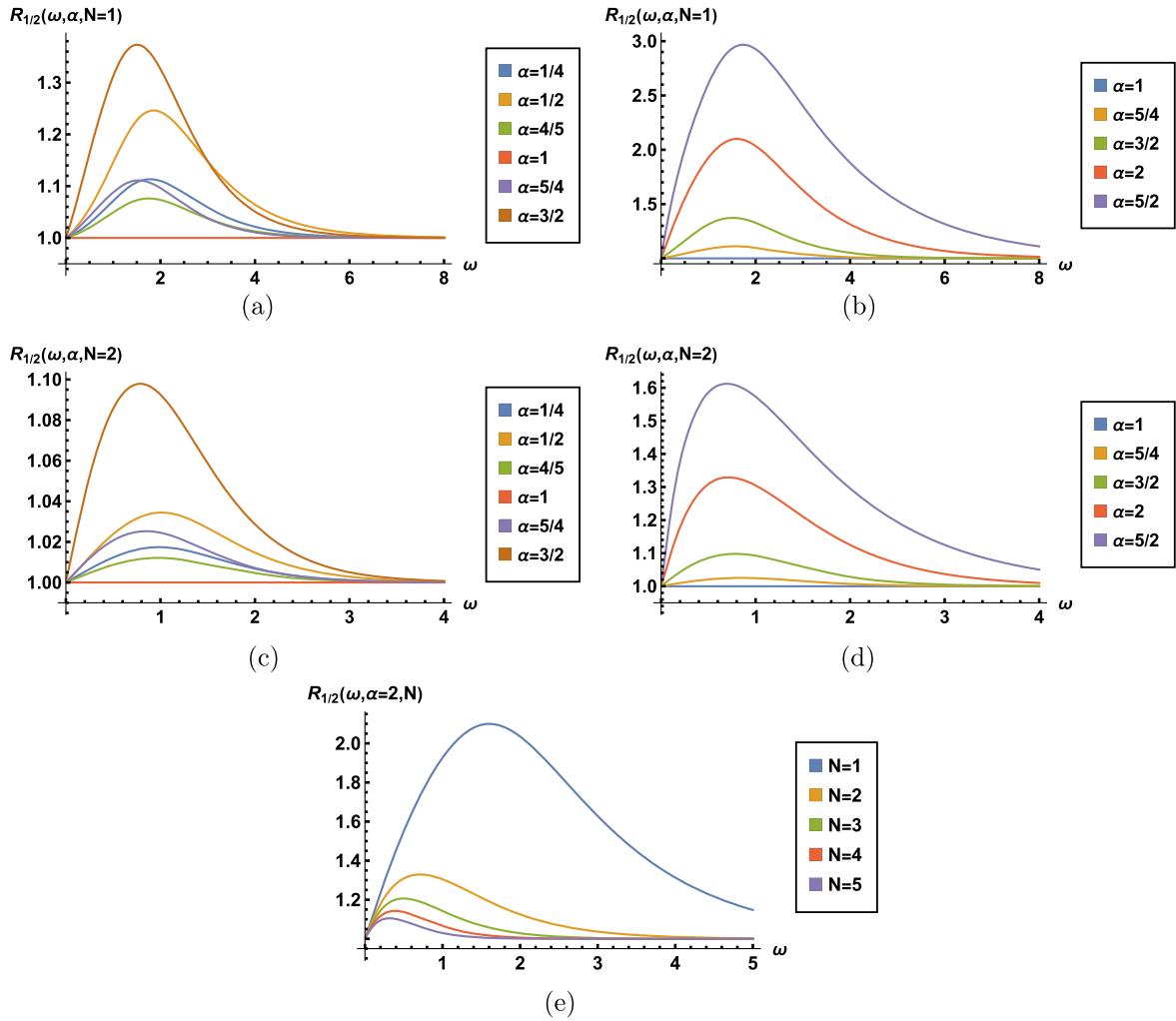
$$\mathrm{Re}(iS_{\mathrm{eff}}) = -\int d^2x \int d\Omega_2 \frac{E^2}{8\pi^3} \beta_{1/2}(\omega, \alpha), \quad (5.10)$$

where

$$\beta_{1/2}(\omega, \alpha) = -\omega \Bigg\{ \sum_{l=0}^{\infty} (2l+1) \ln\left(1 - e^{-\omega(a^2\lambda_l^+ + m^2 a^2)}\right)$$

$$+ \sum_{l=1}^{\infty} (2l+1) \ln\left(1 - e^{-\omega(a^2\lambda_l^- + m^2 a^2)}\right) \Bigg\}, \quad (5.11)$$

and $\lambda_l^{\pm} = \frac{1}{a^2}\left(l^2 + l + 2(\alpha - \frac{1}{2})^2 \pm 2|\alpha - \frac{1}{2}| \sqrt{(l + 1/2)^2 + ((\alpha - \frac{1}{2})^2 - \frac{1}{4})}\right)$ are given in (D12) with $l = 0, 1, 2, \ldots$ for the upper and $l = 1, 2, \ldots$ for the lower sign. Let us also remark that $\lambda_0^+ = \frac{4}{a^2}(\alpha - \frac{1}{2})^2$, yielding a zero mode at $\alpha = \frac{1}{2}$. Note also that $\beta_{1/2}(\omega, \alpha) = \beta_{1/2}(\omega, 1 - \alpha)$.

FIG. 8. Lowest-lying eigenvalues as a function of α.

FIG. 9. $R_{1/2}(\omega, \alpha, N)$ as a function of ω.

Taking the limit $S^2 \to \mathbb{R}^2$, we find

$$
\beta_{1/2}^{\text{flat}}(\omega, \alpha) = -2\omega \Bigg\{ \sum_{l=0}^{\infty} l \ln\left(1 - e^{-\omega(l^2 + 2\alpha^2 + 2|\alpha|\sqrt{l^2 + \alpha^2} + m^2 a^2)}\right) \\
+ \sum_{l=1}^{\infty} l \ln\left(1 - e^{-\omega(l^2 + 2\alpha^2 - 2|\alpha|\sqrt{l^2 + \alpha^2} + m^2 a^2)}\right) \Bigg\}.
$$

$$(5.12)$$

Setting $\frac{l}{a} \to k$ and $\frac{\alpha}{a} \to \beta$ and replacing $\frac{1}{a}\sum_l \frac{l}{a}$ with $\int k\,dk$, we find that $\beta_0^{\text{flat}}(\omega, \alpha) \to \frac{\pi^2}{6} f_{1/2}\left(\frac{\pi}{E}, \beta\right)$, where the last factor is given in (3.11).

Below, we plot the profiles of $\gamma_{1/2}(\omega, \alpha) \equiv \frac{\beta_{1/2}(\omega, \alpha)}{\beta_{1/2}^{\text{flat}}(\omega, \alpha)}$ and $R_{1/2}(\omega, \alpha) \equiv \frac{\beta_{1/2}(\omega, \alpha)}{\beta_{1/2}(\omega, 0)}$. From Fig. 10(a), we see that for $0 \le \alpha \le \frac{1}{2}$ the pair-production amplitude is larger than that of

the flat case. We also see an increasing rate of change with α, which is maximized at $\alpha = \frac{1}{2}$. The latter is essentially due the zero modes in the spectrum at $\alpha = \frac{1}{2}$, which are filled without any energy cost. For $\frac{1}{2} < \alpha \le 1$, relative pair-production rates decrease with increasing α, with the maximal rate reached at $\alpha = 1$. For $\alpha > 1$, $\gamma_{1/2}(\omega, \alpha)$ remains less than the value 1 but slowly converges to it at large ω. We can also note that the overall pair-production amplitudes for $\alpha \ne 0$ are always greater compared to that at $\alpha = 0$. From the plots in Fig. 10(b), we observe that the rate of change in $R_{1/2}(\omega, \alpha)$ increases with α for $0 \le \alpha \le \frac{1}{2}$, decreases for $\frac{1}{2} < \alpha \le 1$, with $R_{1/2}(\omega, \alpha = 1) = 1$ as expected due to the $\alpha \leftrightarrow 1 - \alpha$ symmetry, and increases further above the value 1 for $\alpha > 1$. These features can be readily attributed to the hierarchy among the lowest-lying energy levels $\lambda_l^{\pm}$ and $\lambda_l^{\pm, \text{flat}}$ as seen from Fig. 10(c).
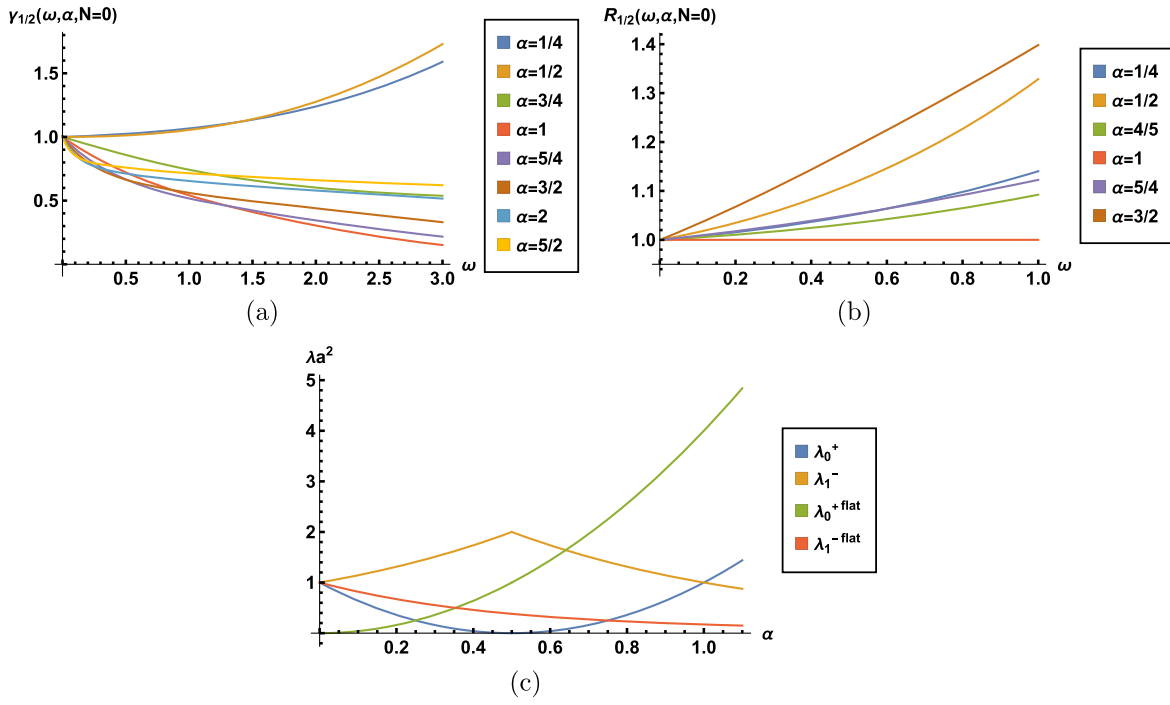
FIG. 10. $\gamma_{1/2}(\omega, \alpha)$ and $R_{1/2}(\omega, \alpha)$ at $N = 0$, Lowest lying energy eigenvalues as function of α (c).

VI. CONCLUSION

In this paper, we have calculated the Schwinger pair-production rates in $\mathbb{R}^{3,1}$ as well as in the positively curved space $S^2 \times \mathbb{R}^{1,1}$ for spin-0 and spin-$\frac{1}{2}$ particles under the influence of an external $SU(2) \times U(1)$ gauge field producing an additional uniform non-Abelian magnetic field besides the usual uniform Abelian electric field. For this purpose, we have obtained the spectrum of the gauged Laplace and Dirac operators on both the flat and the curved geometries and used them to evaluate the Euclidean effective actions, which are Wick rotated at an appropriate stage of the calculation to determine the pair-production amplitudes. From our results, we have seen that, depending on their relative strength, the purely non-Abelian and the Abelian parts of the magnetic field have either a counterplaying or reinforcing role, whose overall effect may be to enhance or suppress the pair-production rates. Positive curvature acts to enhance the latter for spin-0 and suppress it for spin-$\frac{1}{2}$ fields, while the details of the couplings to the purely Abelian and the non-Abelian parts of the magnetic field, which were studied through the dependence of the energy spectra to the

strength of these fields, played a critical role in determining the cumulative effect on the pair-production rates.

APPENDIX A: SPECTRUM OF THE GAUGED LAPLACIAN ON $\mathbb{R}^2$

We have the operator $-D_{(1)}^2 = -(\overrightarrow{\partial} - i\vec{A}_{(1)})^2$, where $\vec{A}_{(1)}$ is valued in the Lie algebra of the gauge group $SU(2) \times U(1)$ and already given in (2.1). The latter yields the field strength

$$
\begin{aligned}
F_{12} &= \partial_1 A_2 - \partial_2 A_1 + i[A_1, A_2] \\
&= \frac{B_1}{2}(\partial_1 x_1 + \partial_2 x_2)\mathbb{1}_2 - i\beta^2[\sigma_2, \sigma_1] \\
&= B_1 \mathbb{1}_2 + 2\beta^2 \sigma_3.
\end{aligned} \tag{A1}
$$

Here, the first term represents an Abelian magnetic field, while the second term is a non-Abelian uniform magnetic field due to a pure $SU(2)$ gauge field. The spectrum of the operator $D_{(1)}^2$ is determined in [28]. Here, we reproduce the result of this paper for convenience. We drop the subscript (1) for ease in notation in what follows. We have

$$
\begin{aligned}
-D^2 &= -(\partial_1 - iA_1)^2 - (\partial_2 - iA_2)^2 \\
&= -(\partial_1^2 - 2iA_1\partial_1 - A_1^2) - (\partial_2^2 - 2iA_2\partial_2 - A_2^2) \\
&= -(\partial_1^2 + \partial_1^2) - i(-B_1 x_2\partial_1 + B_1 x_1\partial_2 - 2\beta\sigma_2\partial_1 + 2\beta\sigma_1\partial_2) + \frac{B_1^2}{4}(x_1^2 + x_2^2) + B_1\beta(x_1\sigma_1 + x_2\sigma_2) + 2\beta^2
\end{aligned}
$$

$$= -4\partial\bar{\partial} + B_1(\bar{z}\,\bar{\partial} - z\partial) + 4\beta(\sigma_-\bar{\partial} - \sigma_+\partial) + \frac{B_1^2}{4}|z|^2 + B_1\beta(z\sigma_- + \bar{z}\sigma_+) + 2\beta^2$$

$$= 2B_1\left(-\frac{2\partial\bar{\partial}}{B_1} + \frac{1}{2}(\bar{z}\,\bar{\partial} - z\partial) + \frac{2\beta}{B_1}(\sigma_-\bar{\partial} - \sigma_+\partial) + \frac{B_1}{8}|z|^2 + \frac{\beta}{2}(z\sigma_- + \bar{z}\sigma_+) + \frac{\beta^2}{B_1}\right)$$

$$= 2B_1\left(a^\dagger a + \sqrt{2}\,\frac{\beta}{\sqrt{B}}(a^\dagger\sigma_+ + a\sigma_-) + \frac{1}{2} + \frac{\beta^2}{B_1}\right)$$

$$= 2B_1\left(a^\dagger a + \sqrt{2}\beta'(a^\dagger\sigma_+ + a\sigma_-) + \frac{1}{2}(1 + 2\beta'^2)\right), \tag{A2}$$

where we have introduced $z = x_1 + ix_2$, $\bar{z} = x_1 - ix_2$, $\partial = \frac{1}{2}(\partial_1 - i\partial_2)$, $\bar{\partial} = \frac{1}{2}(\partial_1 + i\partial_2)$, $\sigma_+ = \frac{1}{2}(\sigma_1 + i\sigma_2)$, and $\sigma_- = \frac{1}{2}(\sigma_1 - i\sigma_2)$ on the fourth line and the creation and annihilation operators in the penultimate line of (A2) via

$$a = \frac{1}{\sqrt{2B_1}}\left(\frac{B_1}{2}z + 2\bar{\partial}\right), \quad a^\dagger = \frac{1}{\sqrt{2B_1}}\left(\frac{B_1}{2}\bar{z} - 2\partial\right). \tag{A3}$$

It can readily be checked that $[a, a^\dagger] = 1$. In the last line in (A2), we have also defined and used the dimensionless non-Abelian magnetic field, which is scaled with respect to the Abelian magnetic field $\beta' \equiv \beta/\sqrt{B_1}$ assuming $B_1 > 0$. In fact, if we change the direction of the Abelian magnetic field, i.e., $B_1 \to -B_1$, we have $-D^2$ retain the form in the last line of (A2) with B_1 replaced with $|B_1|$. Thus, in general, we may write $\beta' \equiv \beta/\sqrt{|B_1|}$.

In matrix form, operator $-D^2$ can be written as

$$-D^2 = 2B_1\begin{pmatrix} a^\dagger a + \frac{1}{2}(1 + 2\beta'^2) & \sqrt{2}\beta' a^\dagger \\ \sqrt{2}\beta' a & a^\dagger a + \frac{1}{2}(1 + 2\beta'^2) \end{pmatrix}. \tag{A4}$$

Clearly, D^2 acts on the Hilbert space $\mathcal{H} = \mathbb{C}^2 \otimes \mathcal{F}$, where $\mathcal{F}$ is the usual Fock space spanned by the eigenstates of the number operator $N = a^\dagger a$. The spectrum of D^2 is obtained in a manner similar to that of the Jaynes-Cummings Hamiltonian [37]. This means that it can be diagonalized in the subspace of $\mathcal{H}_2 \subset \mathcal{H}$ spanned by the states $|n+1, +\rangle$ and $|n, -\rangle$, where n is the eigenvalue of the number operator N and $\pm$ denotes the isospin up and isospin down, respectively. In this subspace, we can write the matrix elements of $D_{(n)}^2$ as

$$-D_{(n)}^2 := 2B_1\begin{pmatrix} n + \frac{1}{2}(1 + 2\beta'^2) & \sqrt{2(n+1)}\beta' \\ \sqrt{2(n+1)}\beta' & n + \frac{1}{2}(1 + 2\beta'^2) \end{pmatrix}. \tag{A5}$$

Diagonalizing $D_{(n)}^2$ yields the eigenvalues

$$\Lambda_n^\pm = 2B_1(n + \beta'^2 \pm \sqrt{2\beta'^2 n + 1/4}), \tag{A6}$$

with $n = 0, 1, 2\ldots$ for the upper and $n = 1, 2, \ldots$ for the lower sign. We note that the ground state is given by $\Lambda_0^+ = 2B_1(\beta'^2 + 1/2)$, using the upper sign in (A6). Let us remark that the corresponding eigenkets of energy are not simultaneous eigenkets of the isospin operator. This is expected, since $-D^2$ does not commute with the third component of the isospin operator σ_3 (nor it does with any component of $\vec{\sigma}$ for that matter). As in the Jaynes-Cummings model [37], a generalized number operator commuting with $-D^2$ can be constructed. Since we do not need these operators, we will not pursue their construction here.

Let us note the two distinct limiting cases. We may take $B_1 \to 0$ (hence, $y = B_1/E \to 0$) and $\beta \to 0$ such that β' is held fixed. This is the limit in which $f_0(y, \beta') \to 1$ as discussed in Sec. II. We may also consider $B_1 \to 0$ and $n_1 \to \infty$ such that $2B_1 n_1 \to k^2$, which gives the configuration with pure non-Abelian magnetic field β. From (A6), we immediately find $\Lambda_n^\pm \to \Lambda_\pm = k^2 + 2\beta^2 \pm 2\beta k$. An alternative and rigorous way to derive the spectrum for this case is presented below.

We may start with the gauged operator $-D^2 = (\vec{\partial} - i\vec{A})^2$, where now $\vec{A} = \vec{A}^{SU(2)}$. We see that $[-D^2, \vec{p}] = 0$, where $\vec{p} = -i\vec{\partial}$. This means that the eigenvalues of $\vec{p}$, say, $\vec{k}$, are good quantum numbers, and we can express the eigenfunctions of $-D^2$ in the form $\psi = \phi(x_1, x_2)e^{i\vec{k}\cdot\vec{x}}$. On the latter, $-D^2$ takes the simple form

$$-D^2 = \begin{pmatrix} k^2 + 2\beta^2 & -2i\beta k_- \\ 2i\beta k_+ & k^2 + 2\beta^2 \end{pmatrix}, \tag{A7}$$

where we have defined $k_\pm = k_1 \pm ik_2$ and $k^2 = k_1^2 + k_2^2$. Diagonalizing this matrix, we find the eigenvalues D^2 are

$$\Lambda_\pm = k^2 + 2\beta^2 \pm 2\beta k. \tag{A8}$$

Finally, we may write the spectrum of $-D_{(1)}^2 - D_{(2)}^2 + m^2$ in $\mathbb{R}^4$ as

$$\text{Spec}(-D_{(1)}^2 - D_{(2)}^2 + m^2) = k^2 + 2\beta^2 \pm 2\beta k + B_2(2n+1) + m^2. \tag{A9}$$

APPENDIX B: SPECTRUM OF THE GAUGED DIRAC OPERATOR ON $\mathbb{R}^2$

Here, we determine the spectrum of the square of the Dirac operator introduced in (3.1). This operator is given as

$$\not{D} = \gamma_i(\partial^i - iA^i), \tag{B1}$$

where we have dropped the subscripts (1) in order not to clutter the notation and the 2×2 γ matrices are given as $\gamma_1 = \tau_1$ and $\gamma_2 = \tau_2$, where τ_1 and τ_2 are the Pauli matrices. $\not{D}$ can be expressed in the 2×2 block matrix form as

$$\not{D} = \begin{pmatrix} 0 & (\partial_1 - i\partial_2) + \frac{B}{2}(-x_1 + ix_2) + \beta(-\sigma_1 + i\sigma_2) \\ (\partial_1 + i\partial_2) + \frac{B}{2}(x_1 + ix_2) + \beta(\sigma_1 + i\sigma_2) & 0 \end{pmatrix}. \tag{B2}$$

Using the notation already introduced in the previous section and (A3) in $\not{D}$, we can write it in the form

$$\not{D} = -\sqrt{2B} \begin{pmatrix} 0 & a^\dagger + 2\beta'\sigma_- \\ -a - 2\beta'\sigma_+ & 0 \end{pmatrix}. \tag{B3}$$

Squaring, we find

$$-\not{D}^2 = 2B \begin{pmatrix} a^\dagger a + \sqrt{2}\beta'(a\sigma_- + a^\dagger\sigma_+) + 2\beta'^2\sigma_-\sigma_+ & 0 \\ 0 & aa^\dagger + \sqrt{2}\beta'(a\sigma_- + a^\dagger\sigma_+) + 2\beta'^2\sigma_+\sigma_- \end{pmatrix}. \tag{B4}$$

Expanding the 2×2 blocks in (B4), we can cast $-\not{D}^2$ in the form

$$-\not{D}^2 = 2B \begin{pmatrix} a^\dagger a & \sqrt{2}\beta' a^\dagger & 0 & 0 \\ \sqrt{2}\beta' a & a^\dagger a + 2\beta'^2 & 0 & 0 \\ 0 & 0 & aa^\dagger + 2\beta'^2 & \sqrt{2}\beta' a^\dagger \\ 0 & 0 & \sqrt{2}\beta' a & aa^\dagger \end{pmatrix}. \tag{B5}$$

Alternatively, we may also note that

$$\begin{aligned} -\not{D}^2 &= -\gamma_i\gamma_j D_i D_j \\ &= -D^2 \mathbb{1}_2 + B_1(\tau_3 \otimes \mathbb{1}_2) + 2\beta^2(\tau_3 \otimes \sigma_3), \end{aligned} \tag{B6}$$

and this immediately yields (B5) upon using (A4).

We may write the eigenvalue equation in the form $-\not{D}^2\Phi = \lambda\Phi$, with $\Phi \equiv (\phi_1, \phi_2, \phi_3, \phi_4)^T$, with T standing for transpose. This leads to the coupled set of operator equations, which can be explicitly written as

$$\omega_c(a^\dagger a\phi_1 + \sqrt{2}\beta' a^\dagger\phi_2) = \lambda\phi_1,$$
$$\omega_c(\sqrt{2}\beta' a\phi_1 + a^\dagger a\phi_2 + 2\beta'^2\phi_2) = \lambda\phi_2,$$
$$\omega_c(aa^\dagger\phi_3 + 2\beta'^2\phi_3 + \sqrt{2}\beta' a^\dagger\phi_4) = \lambda\phi_3,$$
$$\omega_c(\sqrt{2}\beta' a\phi_3 + aa^\dagger\phi_4) = \lambda\phi_4. \tag{B7}$$

We observe that the eigenkets of the operator $-\not{D}^2$ can easily be given in the tensor product space $\mathcal{H} = \mathcal{F} \times \mathbb{C}^2 \otimes \mathbb{C}^2 \equiv \mathcal{F} \otimes \mathbb{C}^4$. Here, the first copy of $\mathbb{C}^2$ stands for the spin and the second copy for the isospin space, and the Fock space is spanned by the eigenstates of the number operator $N = a^\dagger a$ as before. In order to solve (B7), it is almost sufficient to consider the subspace $\mathcal{H}_n \subset \mathcal{H}$ spanned by the states $\{|n+1, +, +\rangle, |n, +, -\rangle, |n, -, +\rangle, |n-1, -, -\rangle\}$, where $n = 0, 1, 2, \ldots$, except for the last ket, for which $n = 1, 2, \ldots$. We may write these kets in the form

$$|n+1, +, +\rangle \equiv \begin{pmatrix} |n+1\rangle \\ 0 \\ 0 \\ 0 \end{pmatrix}, \quad |n, +, -\rangle \equiv \begin{pmatrix} 0 \\ |n\rangle \\ 0 \\ 0 \end{pmatrix},$$

$$|n, -, +\rangle \equiv \begin{pmatrix} 0 \\ 0 \\ |n\rangle \\ 0 \end{pmatrix}, \quad |n-1, -, -\rangle \equiv \begin{pmatrix} 0 \\ 0 \\ 0 \\ |n-1\rangle \end{pmatrix}. \tag{B8}$$

In this subspace, we easily find that

$$-\not{P}^2_{(n)} = 2B \begin{pmatrix} n+1 & \sqrt{2}\beta'\sqrt{n+1} & 0 & 0 \\ \sqrt{2}\beta'\sqrt{n+1} & n+2\beta'^2 & 0 & 0 \\ 0 & 0 & n+1+2\beta'^2 & \sqrt{2}\beta'\sqrt{n} \\ 0 & 0 & \sqrt{2}\beta'\sqrt{n} & n \end{pmatrix}, \tag{B9}$$

and the eigenvalues of $\not{P}^2$ can are then readily computed to be

$$\lambda_n^{\pm} = B_1 \left(1 + 2n + 2\beta'^2 \pm \sqrt{1 + 4\beta'^2(1 + 2n + \beta'^2)}\right), \tag{B10}$$

with each eigenvalue occurring with multiplicity 2. Let us remark that it is legitimate to take $n = 0$ in this expression. This yields $\lambda_0^+ = 2B_1(1 + 2\beta'^2)$, and $\lambda_0^- = 0$. Corresponding eigenkets should be determined with some care. Eigenkets of these states belong to the subspace spanned by the set $\{|0, +, +\rangle, |1, +, +\rangle, |0, +, -\rangle, |0, -, +\rangle\}$, where we note that the state $|0, +, +\rangle$ is not covered by the notation for $\mathcal{H}_n$ introduced above but clearly belongs to the Hilbert space $\mathcal{H}$. We find that the zero mode solutions are

$$|0, +, +\rangle = \begin{pmatrix} |0\rangle \\ 0 \\ 0 \\ 0 \end{pmatrix},$$

$$\frac{(-\sqrt{2}\beta'|1, +, +\rangle + |0, +, -\rangle)}{\sqrt{1 + 2\beta'^2}} = \frac{1}{\sqrt{1 + 2\beta'^2}} \begin{pmatrix} -\sqrt{2}\beta'|1\rangle \\ |0\rangle \\ 0 \\ 0 \end{pmatrix}, \tag{B11}$$

while the eigenkets for the λ_0^+ eigenvalue are

$$|0, +, +\rangle = \begin{pmatrix} 0 \\ 0 \\ |0\rangle \\ 0 \end{pmatrix},$$

$$\frac{(|1, +, +\rangle + \sqrt{2}\beta'|0, +, -\rangle)}{\sqrt{1 + 2\beta'^2}} = \frac{1}{\sqrt{1 + 2\beta'^2}} \begin{pmatrix} |1\rangle \\ \sqrt{2}\beta'|0\rangle \\ 0 \\ 0 \end{pmatrix}. \tag{B12}$$

For $n \geq 1$, we can write the corresponding orthonormal eigenvectors associated with the eigenvalues (B10) in the generic form

$$|\psi^{a_{\pm}}\rangle_n = \frac{1}{\sqrt{a_{\pm}^2 + 1}} (a_{\pm}|n+1, +, +\rangle + |n, +, -\rangle),$$

$$|\psi^{b_{\pm}}\rangle_n = \frac{1}{\sqrt{b_{\pm}^2 + 1}} (b_{\pm}|n, -, +\rangle + |n-1, -, -\rangle), \tag{B13}$$

where

$$a_{\pm} = \frac{1 - 2\beta'^2 \pm \sqrt{1 + 4\beta'^2(1 + 2n + \beta'^2)}}{2\sqrt{2n + 2\beta'}},$$

$$b_{\pm} = \frac{1 + 2\beta'^2 \pm \sqrt{1 + 4\beta'^2(1 + 2n + \beta'^2)}}{2\sqrt{2n}\beta'}. \tag{B14}$$

Here, $\psi_n^{a_{\pm}}$ are the eigenvectors corresponding to the eigenvalues λ_n^+, and $\psi_n^{b_{\pm}}$ are those corresponding to λ_n^-. Let us also note that these states are also simultaneous eigenstates of spin, since $\not{P}^2$ commutes with the spin operator $\gamma_3 \otimes \mathbb{1}_2 = -i\gamma_1\gamma_2 \otimes \mathbb{1}_2 = \tau_3 \otimes \mathbb{1}_2$. $|\psi^{a_{\pm}}\rangle_n$ correspond to spin up and $|\psi^{b_{\pm}}\rangle_n$ to spin down (note that $\pm$ signs are not indicating spin direction). These are not eigenstates of isopin, though, since D^2 and, hence, $\not{P}^2$ do not commute with $\mathbb{1}_2 \otimes \sigma_3$. We may construct a generalized number operator commuting with both $\not{P}^2$ and the isospin operators, but, as this is not necessary for our purposes, we do not pursue it here.

To obtain the eigenvalues of $-\not{P}^2$ in the case of pure non-Abelian magnetic field configuration, we may proceed as follows. Setting $B_1 = 0$ in (B6) yields $-\not{P}^2 = -D^2 + 2\beta^2\tau_3 \otimes \sigma_3$. Since $\not{P}$ commutes with $\vec{p}$, eigenvalues of the latter are good quantum numbers. As before, we may denote these eigenvalues with $\vec{k}$. Thus, $-\not{P}^2$ can be written in matrix form as

$$-\not{P}^2 = \begin{pmatrix} k^2 & -2i\beta k_- & 0 & 0 \\ 2i\beta k_+ & k^2 + 4\beta^2 & 0 & 0 \\ 0 & 0 & k^2 + 4\beta^2 & -2i\beta k_- \\ 0 & 0 & 2i\beta k_+ & k^2 \end{pmatrix}. \tag{B15}$$

Diagonalization gives the eigenvalues

$$\lambda_{\pm} = k^2 + 2\beta^2 \pm 2\beta\sqrt{k^2 + \beta^2}, \tag{B16}$$

with each eigenvalue occurring with multiplicity 2. We remark that, in this case, too, $\not{P}^2$ commutes with the spin operator $\gamma_3 \otimes \mathbb{1}_2 = -i\gamma_1\gamma_2 \otimes \mathbb{1}_2 = \tau_3 \otimes \mathbb{1}_2$ but does not

commute with the isospin. Therefore, the eigenstates of $\not{p}^2$ are simultaneous eigenstates of γ_3 but not σ_3. Observe also that the $\pm$ signs in the eigenvalues are not related with the direction of the spin; in fact, for each sign $\pm$ in $\lambda_\pm$, there is a state with spin up and a state with spin down. Also note that (B16) can also be obtained from (B10) by taking the limit $B_1 \to 0$, $n \to \infty$ such that $2B_1 n \to k^2$.

We can write the spectrum of $-\not{p}^2$ on $\mathbb{R}^4$. Together with the Abelian magnetic field $F_{34} = B_2$ on the second $\mathbb{R}^2$ copy, we have

$$\text{Spec}(-\not{p}^2 + m^2) = \begin{cases} k^2 + 2\beta^2 \pm 2\beta\sqrt{k^2 + \beta^2} + 2nB_2, \\ k^2 + 2\beta^2 \pm 2\beta\sqrt{k^2 + \beta^2} + (2n+2)B_2. \end{cases} \tag{B17}$$

APPENDIX C: SPECTRUM OF THE GAUGED LAPLACIAN ON S^2

Here, we outline the result obtained already in [28]. We consider the following gauged Laplace operator on S^2 with radius a:

$$D^2 = \frac{\vec{\Lambda}^2}{a^2}, \tag{C1}$$

where $\vec{\Lambda}$ is given as

$$\vec{\Lambda} \equiv \vec{r} \times (\vec{p} - \vec{A}), \tag{C2}$$

and the $SU(2) \times U(1)$ gauge field $\vec{A}$ is explicitly written as

$$\vec{A} = \vec{A}_{\text{Abelian}} + \vec{A}_{\text{non-Abelian}}, \qquad \vec{A}_{\text{non-Abelian}} := \alpha \frac{\vec{r} \times \vec{\sigma}}{a^2}. \tag{C3}$$

In (C3), $\vec{A}_{\text{Abelian}}$ stands for the gauge potential of a Dirac monopole with the magnetic charge $N/2$, $N \in \mathbb{Z}$, and $\vec{\sigma}$ are the Pauli matrices spanning the "isospin" $SU(2)$ gauge symmetry. Associated field strength is computed via $\vec{B} = \vec{\nabla} \times \vec{A} - i\vec{A} \times \vec{A}$ and yields a radial magnetic field, which takes the form[17]

$$B = \frac{N}{2a^2} + \left(2\left(\alpha - \frac{1}{2}\right)^2 - \frac{1}{2}\right)\frac{\vec{\sigma} \cdot \hat{r}}{a^2}. \tag{C4}$$

From (C4) it is manifestly seen that B is symmetric under $\alpha \to (\alpha - 1)$, which is a direct consequence of the gauge transformation $UB(\alpha)U = B(\alpha - 1)$, with $U := \vec{\sigma} \cdot \hat{r}$, $U^\dagger = U$, and $U^2 = \mathbb{1}_2$.

We may write, in the same manner as in the Landau problem on S^2 [38],

---

[17]Note that the choice of gauge for $\vec{A}_{\text{Abelian}}$ is immaterial for our purposes.

$$\vec{\Lambda} = \vec{L} + \frac{N}{2}\hat{r} + \alpha(\vec{\sigma} - (\vec{\sigma} \cdot \hat{r})\hat{r})$$
$$= \vec{\Lambda}_{\text{Abelian}} + \alpha(\vec{\sigma} - (\vec{\sigma} \cdot \hat{r})\hat{r}). \tag{C5}$$

where $\vec{L} = \vec{\Lambda}_{\text{Abelian}} - \frac{N}{2}\hat{r}$ is the angular momentum solely generated by the charge-Dirac monopole system. The total angular momentum operator is found by adding the contribution of the isospin:

$$\vec{J} = \vec{L} + \frac{\vec{\sigma}}{2} = \vec{r} \times (\vec{p} - \vec{A}_{\text{Abelian}}) - \frac{N}{2}\hat{r} + \frac{\vec{\sigma}}{2},$$
$$= \vec{\Lambda}_{\text{Abelian}} - \frac{N}{2}\hat{r} + \frac{\vec{\sigma}}{2},$$
$$= \vec{\Lambda} - \alpha(\vec{\sigma} - (\vec{\sigma} \cdot \hat{r})\hat{r}) - \frac{N}{2}\hat{r} + \frac{\vec{\sigma}}{2}. \tag{C6}$$

We have

$$\left(\vec{J} + \left(\alpha - \frac{1}{2}\right)\vec{\sigma}\right)^2 = \left(\vec{\Lambda} + \alpha\left(\vec{\sigma} \cdot \hat{r} - \frac{N}{2}\right)\hat{r}\right)^2. \tag{C7}$$

Upon using $\vec{\Lambda} \cdot \hat{r} = 0 = \hat{r} \cdot \vec{\Lambda}$ and rearranging the terms, this yields

$$D^2 = \frac{1}{a^2}\left(\vec{J}^2 + \frac{1}{4} - \frac{N^2}{4} + 2\left(\alpha - \frac{1}{2}\right)^2 - \frac{1}{2} + 2\left(\alpha - \frac{1}{2}\right)\right.$$
$$\left. \times \left(\vec{J} \cdot \vec{\sigma} - \frac{1}{2} + \frac{N}{2}\vec{\sigma} \cdot \hat{r}\right) + \frac{N}{2}\vec{\sigma} \cdot \hat{r}\right). \tag{C8}$$

It is useful to define $X := 2(\alpha - \frac{1}{2})(\vec{J} \cdot \vec{\sigma} - \frac{1}{2} + \frac{N}{2}\vec{\sigma} \cdot \hat{r}) + \frac{N}{2}\vec{\sigma} \cdot \hat{r}$. It squares to

$$X^2 = 4\left(\alpha - \frac{1}{2}\right)^2\left(\vec{J}^2 + \frac{1}{4}\right) - \left(\left(\alpha - \frac{1}{2}\right)^2 - \frac{1}{4}\right)N^2, \tag{C9}$$

which is diagonal in the total angular momentum basis. $\vec{J}$ carries the angular momentum values given by the tensor product $j \equiv l \otimes \frac{1}{2} = (l - 1/2) \oplus (l + 1/2)$, where l is the angular momentum of the charge monopole system. Setting $l = n_1 + \frac{N}{2}$, possible values of j are $j = n_1 + \frac{N-1}{2}$ and $j = n_1 + \frac{N+1}{2}$ with $n_1 = 0, 1, 2, \ldots$ and $N = 1, 2, \ldots$. To be more precise, the Hilbert space becomes block diagonal in the total angular momentum basis and splits into the direct sum of IRRs:

$$\left(\frac{N-1}{2}\right) \oplus \mathbf{2}\left(\frac{N+1}{2}\right) \oplus \mathbf{2}\left(\frac{N+3}{2}\right) \oplus \cdots, \tag{C10}$$

where the coefficients written in bold typeface denote the multiplicities of the respective IRRs. Except the first IRR,

which corresponds to the ground state with $n_1 = 0$, each IRR occurs twice. In the $j = n_1 + \frac{N+1}{2}$ branch, we may shift $n_1 \rightarrow n_1 - 1$ and write the spectrum of D^2 as

$$\Lambda_{n_1}^{\pm}(\alpha) = \frac{1}{a^2}\left(n_1(N + n_1) + 2\left(\alpha - \frac{1}{2}\right)^2 - \frac{1}{2}\right.$$
$$\left. \pm \sqrt{4\left(\alpha - \frac{1}{2}\right)^2(n_1 + N)n_1 + \frac{N^2}{4}}\right). \quad \text{(C11)}$$

We observe that $\Lambda_{n_1}^{\pm}(\alpha) = \Lambda_{n_1}^{\pm}(1 - \alpha)$. Ground state energy is given by $\Lambda_0^+ = \frac{1}{a^2}(2(\alpha - \frac{1}{2})^2 - \frac{1}{2} + \frac{N}{2})$, where we have

taken $n_1 = 0$ and the $+$ sign in front of the square root term. The latter follows from the continuity of the energy spectrum as $\alpha \rightarrow 0$ matching the ground state energy of the Landau problem on the sphere [38]. Hence, we have $n_1 = 0, 1, 2, \ldots$ for $\Lambda_{n_1}^+$ and $n_1 = 1, 2, \ldots$ for $\Lambda_{n_1}^-$. Let us immediately note that taking the limit $N \rightarrow \infty$, $a \rightarrow \infty$, and $\alpha \rightarrow \infty$, such that $B_1 = \frac{N}{2a^2}$, $\beta^2 = \frac{\alpha^2}{a^2}$ fixed, and $\beta'^2 = \frac{\beta^2}{B_1}$, yields the spectrum of D^2 on $\mathbb{R}^2$ given in (A6) as expected.

It is straightforward to see that D^2 and $\vec{J}$ commute. We may note that the only nontrivial commutators are $[J_i, \vec{\sigma} \cdot \hat{r}]$ and $[J_i, \vec{J} \cdot \vec{\sigma}]$. These vanish as the following calculations demonstrate:

$$[J_i, \vec{\sigma} \cdot \hat{r}] = \left[\epsilon_{ijk}r_j(p_k - A_k) - \frac{N}{2}\frac{r_i}{\sqrt{r_l r_l}} + \frac{\sigma_i}{2}, \frac{\sigma_n r_n}{\sqrt{r_m r_m}}\right]$$

$$= \epsilon_{ijk}\left[r_j(p_k - A_k), \frac{\sigma_n r_n}{\sqrt{r_m r_m}}\right] - \frac{N}{2}\left[\frac{r_i}{\sqrt{r_l r_l}}, \frac{\sigma_n r_n}{\sqrt{r_m r_m}}\right] + \frac{r_n}{2r}[\sigma_i, \sigma_n]$$

$$= \epsilon_{ijk}r_j\left[(p_k - A_k), \frac{\sigma_n r_n}{\sqrt{r_m r_m}}\right] + \epsilon_{ijk}\left[r_j, \frac{\sigma_n r_n}{\sqrt{r_m r_m}}\right](p_k - A_k) + \frac{r_n}{2r}[\sigma_i, \sigma_n]$$

$$= \epsilon_{ijk}r_j\left[p_k, \frac{\sigma_n r_n}{\sqrt{r_m r_m}}\right] + \frac{r_n}{2r}[\sigma_i, \sigma_n]$$

$$= -i\epsilon_{ijk}r_j\sigma_n\frac{r^2\delta_{nk} - r_n r_k}{r^3} + \frac{r_n}{2r}[\sigma_i, \sigma_n]$$

$$= -i\epsilon_{ijk}\frac{r_j}{r}\sigma_n\delta_{nk} + \frac{r_n}{2r}[\sigma_i, \sigma_n]$$

$$= -i\epsilon_{ijk}\frac{r_j}{r}\sigma_k + \frac{r_n}{2r}2i\epsilon_{ink}\sigma_k$$

$$= 0, \quad \text{(C12)}$$

$$[J_i, J_j\sigma_j] = \left[L_i + \frac{1}{2}\sigma_i, \left(L_j + \frac{1}{2}\sigma_j\right)\sigma_j\right]$$

$$= [L_i, L_j]\sigma_j + L_j[L_i, \sigma_j] + \frac{1}{2}[\sigma_i, L_j]\sigma_j + \frac{1}{2}L_j[\sigma_i, \sigma_j]$$

$$= [L_i, L_j]\sigma_j + \frac{1}{2}L_j[\sigma_i, \sigma_j]$$

$$= i\epsilon_{ijk}(L_k\sigma_j + L_j\sigma_k)$$

$$= 0. \quad \text{(C13)}$$

Therefore, we conclude that each energy level in (C11) is $(2j + 1)$-fold degenerate. The degeneracy of each branch of these energy levels is, thus, the same as that of the Landau problem on the sphere [38]. In particular, the ground level with energy Λ_0^+ is N-fold degenerate.

In the absence of the Abelian magnetic field, i.e., setting $N = 0$, the operator D^2 takes the form

$$D^2 = \frac{1}{a^2}\left(J^2 + \frac{1}{4} + 2\left(\alpha - \frac{1}{2}\right)^2 - \frac{1}{2} + 2\left(\alpha - \frac{1}{2}\right)(\vec{J} \cdot \vec{\sigma} - 1/2)\right), \quad \text{(C14)}$$

while $X = 2(\alpha - \frac{1}{2})(\vec{J} \cdot \vec{\sigma} - 1/2) = 2(\alpha - \frac{1}{2})(\vec{J}^2 - \vec{L}^2 + 1/4)$ with the eigenvalues $2(\alpha - \frac{1}{2})(l + 1)$ for the IRR $j = l + 1/2$ ($l = 0, 1, 2, 3, \ldots$) and $-2(\alpha - \frac{1}{2})l$ for the IRR

$j = l - 1/2$ ($l = 1, 2, 3, \ldots$). Thus, the Hilbert space splits into the direct sum

$$2\left(\frac{1}{2}\right) \oplus 2\left(\frac{3}{2}\right) \oplus \cdots. \tag{C15}$$

The spectrum of D^2 can be written as

$$\Lambda^+_{l,N=0} = \frac{1}{a^2}\left((l+1)^2 + 2\left(\alpha - \frac{1}{2}\right)^2 - \frac{1}{2} + 2\left(\alpha - \frac{1}{2}\right)(l+1)\right),$$
$$l = 0, 1, 2 \ldots, \tag{C16a}$$

$$\Lambda^-_{l,N=0} = \frac{1}{a^2}\left(l^2 + 2\left(\alpha - \frac{1}{2}\right)^2 - \frac{1}{2} - 2\left(\alpha - \frac{1}{2}\right)l\right),$$
$$l = 1, 2 \ldots. \tag{C16b}$$

Note that, as $\alpha \to 0$, we have that $D^2 = \vec{L}^2/a^2$, which has the spectrum $\frac{1}{a^2} l(l+1)$, $l = 0, 1, 2, \ldots$, and $\Lambda^+_{l,N=0}$ already gives a zero mode at $l = 0$. We remark that, in this limit, D^2 becomes independent of $\vec{J}^2$ as expected, and not only in $\Lambda^+_{l,N=0}$ but also in $\Lambda^-_{l,N=0}$ we have $l = 0, 1, 2, \ldots$.

Shifting $l \to l - 1$ in $\Lambda^+_{l,N=0}$, we may write the spectrum more compactly as $\Lambda^\pm_{l,N=0}(\alpha) = \frac{1}{a^2}(l^2 + 2(\alpha - \frac{1}{2})^2 - \frac{1}{2} \pm 2(\alpha - \frac{1}{2})l)$ with $l = 1, 2 \ldots$ for $\alpha \neq 0$, while for $\alpha = 0$ only, $l = 0, 1, \ldots$ for the lower sign. Let us also remark that $\Lambda^\pm_{l,N=0}(\alpha) = \Lambda^\mp_{l,N=0}(1 - \alpha)$ indicates that the spectrum remains the same under $\alpha \leftrightarrow 1 - \alpha$. As consequence, at $\alpha = 1$, $\Lambda^-_{l,N=0}$ is a zero mode at $l = 1$.

Taking $l \to \infty$, $a \to \infty$, $\gamma \to \infty$, such that $\frac{l}{a} \to k$ and $\frac{\alpha^2}{a^2} \to \beta$ remain finite, we obtain the spectrum on $\mathbb{R}^2$ given in (A8).

APPENDIX D: SPECTRUM OF THE GAUGED DIRAC OPERATOR ON S^2

We consider the Dirac operator in the background of the total magnetic field introduced in (C3). This Dirac operator can be written as $\slashed{D} = \frac{1}{a}(\vec{\tau} \cdot \vec{\Lambda} + 1)$, where $\vec{\tau}$ are the Pauli matrices, spanning the Clifford algebra $\{\tau_i, \tau_j\} = 2\delta_{ij}$, and $\vec{\Lambda}$ is defined as previously in (C2). For the square of the Dirac operator, we have

$$\begin{aligned}
a^2 \slashed{D}^2 &= (\vec{\tau} \cdot \vec{\Lambda} + 1)^2 \\
&= (\vec{\tau} \cdot \vec{\Lambda})^2 + 2\vec{\tau} \cdot \vec{\Lambda} + 1 \\
&= \tau_i \tau_j \Lambda_i \Lambda_j = (\delta_{ij} + i\epsilon_{ijk}\tau_k)\Lambda_i\Lambda_j + 2\vec{\tau} \cdot \vec{\Lambda} + 1 \\
&= \Lambda^2 + \frac{i}{2}\epsilon_{ijk}[\Lambda_i, \Lambda_j]\tau_k + 2\vec{\tau} \cdot \vec{\Lambda} + 1 \\
&= \Lambda^2 + \frac{i}{2}\epsilon_{ijk}\left[L_i + \frac{N}{2}\hat{r}_i + \alpha(\sigma_i - \sigma_n\hat{r}_n\hat{r}_i), L_j + \frac{N}{2}\hat{r}_j + \alpha(\sigma_j - \sigma_m\hat{r}_m\hat{r}_j)\right]\tau_k + 2\vec{\tau} \cdot \vec{\Lambda} + 1 \\
&= \Lambda^2 + \frac{i}{2}\epsilon_{ijk}\left([L_i, L_j] + \frac{N}{2}[L_i, \hat{r}_j] + \frac{N}{2}[\hat{r}_i, L_j] - \alpha[L_i, \sigma_m\hat{r}_m\hat{r}_j] - \alpha[\sigma_n\hat{r}_n\hat{r}_i, L_j]\right. \\
&\quad \left. - \alpha^2[\sigma_i, \sigma_m\hat{r}_m\hat{r}_j] - \alpha^2[\sigma_n\hat{r}_n\hat{r}_i, \sigma_j] + \alpha^2[\sigma_i, \sigma_j] + \alpha^2[\sigma_n\hat{r}_n\hat{r}_i, \sigma_m\hat{r}_m\hat{r}_j]\right)\tau_k + 2\vec{\tau} \cdot \vec{\Lambda} + 1 \\
&= \Lambda^2 + \frac{i}{2}\epsilon_{ijk}\left([L_i, L_j] + \frac{N}{2}[L_i, \hat{r}_j] + \frac{N}{2}[\hat{r}_i, L_j] - \alpha\sigma_m[L_i, \hat{r}_m\hat{r}_j] - \alpha\sigma_n[\hat{r}_n\hat{r}_i, L_j]\right. \\
&\quad \left. - \alpha^2\hat{r}_m\hat{r}_j[\sigma_i, \sigma_m] - \alpha^2\hat{r}_n\hat{r}_i[\sigma_n, \sigma_j] + \alpha^2[\sigma_i, \sigma_j] + \alpha^2\hat{r}_n\hat{r}_i\hat{r}_m\hat{r}_j[\sigma_n, \sigma_m]\right)\tau_k + 2\vec{\tau} \cdot \vec{\Lambda} + 1 \\
&= \Lambda^2 + \vec{\tau} \cdot \vec{\Lambda} - \frac{N}{2}\vec{\tau} \cdot \hat{r} + 1 - 2\left(\left(\alpha - \frac{1}{2}\right)^2 - \frac{1}{4}\right)(\vec{\tau} \cdot \hat{r})(\vec{\sigma} \cdot \hat{r}). \tag{D1}
\end{aligned}$$

Using $\vec{J} = \vec{L} + \frac{\vec{\sigma}}{2}$, we have the intermediate expression

$$a^2 \slashed{D}^2 = J^2 + 2\left(\alpha - \frac{1}{2}\right)\vec{J} \cdot \vec{\sigma} + \frac{3}{4} - 3\alpha + 2\alpha^2 + N\alpha\vec{\sigma} \cdot \hat{r} - \frac{N^2}{4} + \vec{\tau} \cdot \vec{J}$$
$$+ \left(\alpha - \frac{1}{2}\right)\vec{\tau} \cdot \vec{\sigma} - 2\alpha\left(\alpha - \frac{1}{2}\right)(\vec{\sigma} \cdot \hat{r})(\vec{\tau} \cdot \hat{r}) + 1. \tag{D2}$$

At this stage, we may introduce the total angular momentum operator $\vec{K}$ and the operator $\vec{\tau} \cdot \vec{J}$ as

$$\vec{K} = \vec{J} + \frac{\vec{\tau}}{2} = \vec{L} + \frac{\vec{\sigma}}{2} + \frac{\vec{\tau}}{2}, \tag{D3a}$$

$$\vec{\tau} \cdot \vec{J} = K^2 - J^2 - \frac{\tau^2}{4}. \tag{D3b}$$

These allow us to express $\not{p}^2$ in the form

$$a^2 \not{p}^2 = K^2 - \left(\frac{N^2}{4} - 2\left(\alpha - \frac{1}{2}\right)^2\right)$$
$$+ \left[2\left(\alpha - \frac{1}{2}\right)\left(\vec{K} \cdot \vec{\sigma} - \frac{1}{2}\right) + N\alpha\vec{\sigma} \cdot \hat{r}\right.$$
$$\left. - 2\alpha\left(\alpha - \frac{1}{2}\right)(\vec{\sigma} \cdot \hat{r})(\vec{\tau} \cdot \hat{r})\right]. \tag{D4}$$

In this expression, the first two terms are already diagonal, but we have to diagonalize the operator in the brackets $\chi := 2(\alpha - \frac{1}{2})(\vec{K} \cdot \vec{\sigma} - \frac{1}{2}) + N\alpha\vec{\sigma} \cdot \hat{r} - 2\alpha(\alpha - \frac{1}{2})(\vec{\sigma} \cdot \hat{r})(\vec{\tau} \cdot \hat{r})$. Squaring it, we find

$$\chi^2 = 4\left(\alpha - \frac{1}{2}\right)^2\left(K^2 + \frac{1}{4}\right) - \left(\left(\alpha - \frac{1}{2}\right)^2 - \frac{1}{4}\right)$$
$$\times \left(N^2 - 4\left(\alpha - \frac{1}{2}\right)^2\right), \tag{D5}$$

which is diagonal in the total angular momentum basis. We let l represent the angular momentum of the charge-Dirac monopole system as before. Then, the total angular momentum K could take on the possible values given by the tensor product

$$k \equiv l \otimes \frac{1}{2} \otimes \frac{1}{2}$$
$$\equiv (l+1) \oplus 2l \oplus (l-1)$$
$$= \left(n_1 + \frac{N}{2} + 1\right) \oplus 2\left(n_1 + \frac{N}{2}\right) \oplus \left(n_1 + \frac{N}{2} - 1\right), \tag{D6}$$

where in the last line we have used $l = n_1 + \frac{N}{2}$, with $N = 1, 2, \ldots$ and $n_1 = 0, 1, 2, \ldots$ except in the last direct summand at $N = 1$ for which $n_1 = 1, 2, \ldots$. Thus, at a given orbital angular momentum, the spectrum of $\not{p}^2$ has four distinct eigenvalues, and we may express them as

$$\lambda_{n_1+1}(\alpha) = \frac{1}{a^2}\left(\xi_{n_1+1} + \left(\alpha - \frac{1}{2}\right)^2 - \sqrt{4\left(\alpha - \frac{1}{2}\right)^2 \xi_{n_1+1} + \frac{N^2}{4}}\right), \tag{D7a}$$

$$\lambda_{n_1}^{\pm}(\alpha) = \frac{1}{a^2}\left(\xi_{n_1} + \left(\alpha - \frac{1}{2}\right)^2 \pm \sqrt{4\left(\alpha - \frac{1}{2}\right)^2 \xi_{n_1} + \frac{N^2}{4}}\right), \tag{D7b}$$

$$\lambda_{n_1-1}(\alpha) = \frac{1}{a^2}\left(\xi_{n_1-1} + \left(\alpha - \frac{1}{2}\right)^2 + \sqrt{4\left(\alpha - \frac{1}{2}\right)^2 \xi_{n_1-1} + \frac{N^2}{4}}\right), \tag{D7c}$$

where

$$\xi_{n_1}(\alpha) = \left(n_1 + \frac{1}{2}\right)^2 + N\left(n_1 + \frac{1}{2}\right) + \left(\left(\alpha - \frac{1}{2}\right)^2 - \frac{1}{4}\right), \tag{D8}$$

and each eigenvalue being $(2k + 1)$-fold degenerate with $k = l + 1, l, l - 1$ as given in (D6). Clearly, the spectrum is symmetric under $\alpha \leftrightarrow 1 - \alpha$. For $N \geq 2$, this spectrum has zero modes at the branches $\lambda_{n_1}^-$ and λ_{n_1-1} for $n_1 = 0$. For $N = 1$, we have from (D7c) that the set of eigenvalues λ_{n_1-1} starts with $n_1 = 1$, since the IRR $(n_1 + \frac{N}{2} - 1)$ does not exist at $N = 1, n_1 = 0$, meaning that this branch does not include a zero mode, while the spectrum of $\not{p}^2$ retains the zero mode from the branch $\lambda_{n_1}^-$. Let us recall that at $N = 0$ and $\alpha = 0$, i.e., in the absence of the entire magnetic background, the Dirac operator on S^2 has no zero modes. In a similar manner, for the present problem, absence of the zero mode in the branch λ_{n_1-1} at $N = 1$ can, therefore, be understood as the insufficient contribution of the Dirac monopole flux to the total angular momentum to compensate the total spin and isospin down contributions to the latter.

To make these results manifestly clear, first, let us note that, as $\alpha \to 0$, we have

$$\chi|_{\alpha=0} =: \chi_0 = -(\vec{K} \cdot \vec{\sigma} - 1/2) = -(\vec{K}^2 - \vec{M}^2 + 1/4), \tag{D9}$$

where $\vec{M} = \vec{L} + \frac{\vec{\tau}}{2}$ and from (D4) we immediately recover $a^2\not{p}^2 = \vec{M}^2 - \frac{N^2}{4} + \frac{1}{4}$, which is the standard form of the Dirac operator on S^2 in the presence of the Dirac monopole [39] and manifestly independent of $\vec{K}^2$ and dependent on $\vec{M}^2$. Its spectrum can easily be written and matches with that obtained from (D7) by taking $\alpha \to 0$. This yields one copy of the set of eigenvalues $(n_1 + 1)^2 + (n_1 + 1)N$ and $n_1^2 + n_1 N$ for isospin up and one for isospin down with $n_1 = 0, 1, \ldots$ and $N \geq 1$, with the zero modes at $n_1 = 0$ from the latter set for both the isospin up and down configurations.

In the present case, for the branch λ_{n_1-1} at $n_1 = 0$ and $N \geq 2$, we have to be careful about the square root term in the rhs of (D7c). In this case, we find that χ^2 has the

eigenvalue $(\frac{N}{2} - 2(\alpha - \frac{1}{2})^2)^2$. Above, we have already seen how the spectrum and, in particular, the zero modes of $\not{D}^2$ are obtained in the $\alpha \to 0$ limit. By continuity in α, we conclude that the correct eigenvalue of χ is $\frac{N}{2} - 2$ $(\alpha - \frac{1}{2})^2$ (which could be positive or negative depending on the values of N and α), and this yields the zero mode in the indicated branch. In other words, for $n_1 = 0$ and $N \geq 2$, $\sqrt{4(\alpha - \frac{1}{2})^2 \xi_{n_1-1} + N^2/4}$ in (D7c) is replaced with $\frac{N}{2} - 2(\alpha - \frac{1}{2})^2$.

We may note that, taking the limit $N \to \infty$, $a \to \infty$, and $\alpha \to \infty$, such that $B_1 = \frac{N}{2a^2}$, $\beta^2 = \frac{\alpha^2}{a^2}$ kept fixed, and $\beta'^2 = \frac{\beta^2}{B_1}$, yields the spectrum of $\not{D}^2$ on $\mathbb{R}^2$ given in (B10) as expected.

In the absence of the Abelian magnetic field, $\not{D}^2$ takes the form

$$\not{D}^2 = K^2 + 2\left(\alpha - \frac{1}{2}\right)^2 + \chi, \qquad \text{(D10)}$$

and $\chi = 2(\alpha - \frac{1}{2})(\vec{K} \cdot \vec{\sigma} - \frac{1}{2}) - 2((\alpha - \frac{1}{2})^2 - \frac{1}{4})(\vec{\sigma} \cdot \hat{r})(\vec{\tau} \cdot \hat{r})$, with the eigenvalues $\pm 2|\alpha - \frac{1}{2}|((k + \frac{1}{2})^2 + (\alpha - \frac{1}{2})^2 - \frac{1}{4})$ as easily seen from (D5) after setting $N = 0$ in that expression. Total angular momentum $\vec{K}$ could carry the irreducible representations: $(l + 1), l, l, (l - 1)$ with $l = 0, 1, \ldots$ for the first two of the IRRs and $l = 1, 2, \ldots$ for the remaining two. The spectrum of $\not{D}^2$ becomes

$$\lambda_{l+1}(\alpha) = \frac{1}{a^2}\left(l^2 + 3l + 2 + 2\left(\alpha - \frac{1}{2}\right)^2 - 2\left|\alpha - \frac{1}{2}\right|\sqrt{(l + 3/2)^2 + \left(\left(\alpha - \frac{1}{2}\right)^2 - \frac{1}{4}\right)}\right), \qquad \text{(D11a)}$$

$$\lambda_l^\pm(\alpha) = \frac{1}{a^2}\left(l^2 + l + 2\left(\alpha - \frac{1}{2}\right)^2 \pm 2\left|\alpha - \frac{1}{2}\right|\sqrt{(l + 1/2)^2 + \left(\left(\alpha - \frac{1}{2}\right)^2 - \frac{1}{4}\right)}\right), \qquad \text{(D11b)}$$

$$\lambda_{l-1}(\alpha) = \frac{1}{a^2}\left(l^2 - l + 2\left(\alpha - \frac{1}{2}\right)^2 + 2\left|\alpha - \frac{1}{2}\right|\sqrt{(l - 1/2)^2 + \left(\left(\alpha - \frac{1}{2}\right)^2 - \frac{1}{4}\right)}\right), \qquad \text{(D11c)}$$

where $l = 0, 1, \ldots$ for λ_{l+1} and λ_l^+ and $l = 1, 2, \ldots$ for λ_l^- and λ_{l-1}. Quite interestingly, we notice that $\lambda_l^+|_{l=0} = \lambda_{l-1}|_{l=1} = 4(\alpha - \frac{1}{2})^2$, from which we make the observation that these states produce zero modes at the special value $\alpha = \frac{1}{2}$ of the non-Abelian gauge coupling. Taking $l \to l + 1$ in λ_{l-1} yields the same as λ_l^+ and $l \to l - 1$ in λ_{l+1} yields the same as λ_l^-. Thus, we may write the spectrum in (D11a) as

$$\lambda_l^\pm(\alpha) = \frac{1}{a^2}\left(l^2 + l + 2\left(\alpha - \frac{1}{2}\right)^2 \pm 2|\alpha - \frac{1}{2}|\sqrt{(l + 1/2)^2 + \left(\left(\alpha - \frac{1}{2}\right)^2 - \frac{1}{4}\right)}\right), \qquad \text{(D12)}$$

with $l = 0, 1, 2, \ldots$ for the upper and $l = 1, 2, \ldots$ for the lower sign and each eigenvalue occurring with multiplicity 2. We see that $\lambda_l^\pm(\alpha) = \lambda_l^\pm(1 - \alpha)$; i.e., the spectrum remains the same under $\alpha \leftrightarrow 1 - \alpha$. Taking $\alpha \to 0$, we obtain from (D11a) the eigenvalues $(l + 1)^2$ with $l = 0, 1, \ldots$, and this matches with the spectrum of $\not{D}^2$ on S^2. These two facts uniquely fix the sign choices in front of the square root term in (D12).

Finally, we note that, with $l \to \infty$, $a \to \infty$, and $\alpha \to \infty$, such that $\frac{l}{a} \to k$, $\frac{\alpha^2}{a^2} \to \beta^2$ remaining finite, we obtain the spectrum on $\mathbb{R}^2$ given in (B16).

---

[1] H. Casimir, On the attraction between two perfectly conducting plates, Indagat. Math **10**, 261 (1948).

[2] J. Schwinger, On gauge invariance and vacuum polarization, Phys. Rev. **82**, 664 (1951).

[3] A. Ringwald, Pair production from vacuum at the focus of an x-ray free electron laser, Phys. Lett. B **510**, 107 (2001).

[4] A. Fedotov, A. Ilderton, F. Karbstein, B. King, D. Seipt, H. Taya, and G. Torgrimsson, Advances in QED with intense background fields, Phys. Rep. **1010**, 1 (2023).

[5] F. Sauter, Über den atomaren Photoeffekt bei großer Härte der anregenden Strahlung, Ann. Phys. (Berlin) **401**, 217 (1931).

[6] W. Heisenberg and H. Euler, Folgerungen aus der dirac-schen theorie des positrons, Z. Phys. **98**, 714 (1936).

[7] E. Brezin and C. Itzykson, Pair production in vacuum by an alternating field, Phys. Rev. D **2**, 1191 (1970).

[8] G. Dunne and T. Hall, QED effective action in time dependent electric backgrounds, Phys. Rev. D **58**, 105022 (1998).

[9] F. Hebenstreit, R. Alkofer, and H. Gies, Pair production beyond the Schwinger formula in time-dependent electric fields, Phys. Rev. D **78**, 061701 (2008).

[10] G. Dunne and C. Schubert, Worldline instantons and pair production in inhomogenous fields, Phys. Rev. D **72**, 105004 (2005).

[11] H. Gies and K. Klingmüller, Pair production in inhomogeneous fields, Phys. Rev. D **72**, 065001 (2005).

[12] R. Schützhold, H. Gies, and G. Dunne, Dynamically assisted Schwinger mechanism, Phys. Rev. Lett. **101**, 130404 (2008).

[13] K. Hattori, K. Itakura, and S. Ozaki, Strong-field physics in QED and QCD: From fundamentals to applications, Prog. Part. Nucl. Phys. **133**, 104068 (2023).

[14] A. Berdyugin *et al.*, Out-of-equilibrium criticalities in graphene superlattices, Science **375**, 430 (2022).

[15] A. Schmitt, P. Vallet, D. Mele, M. Rosticher, T. Taniguchi, K. Watanabe, E. Bocquillon, G. Fève, J. Berroir, C Voisin, J. Cayssol, M. Goerbig, J. Troost, E. Baudin, and B. Plaçais, Mesoscopic Klein-Schwinger effect in graphene, Nat. Phys. **19**, 830 (2023).

[16] D. Karabali, S. Kürkçüoğlu, and V. Nair, Magnetic field and curvature effects on pair production. I. Scalars and spinors, Phys. Rev. D **100**, 065005 (2019).

[17] D. Karabali, S. Kürkçüoğlu, and V. Nair, Magnetic field and curvature effects on pair production. II. Vectors and implications for chromodynamics, Phys. Rev. D **100**, 065006 (2019).

[18] L. Brown and W. Weisberger, Vacuum polarization in uniform non-Abelian gauge fields, Nucl. Phys. **B157**, 285 (1979).

[19] P. Hasenfratz and G. 't Hooft, Fermion-boson puzzle in a gauge theory, Phys. Rev. Lett. **36**, 1119 (1976).

[20] R. Jackiw and C. Rebbi, Spin from isospin in a gauge theory, Phys. Rev. Lett. **36**, 1116 (1976).

[21] A. P. Balachandran and G. Immirzi, The Fuzzy Ginsparg-Wilson algebra: A solution of the fermion doubling problem, Phys. Rev. D **68**, 065023 (2003).

[22] A. Yildiz and P. H. Cox, Vacuum behavior in quantum chromodynamics, Phys. Rev. D **21**, 1095 (1980); M. Claudson, A. Yildiz, and P. H. Cox, Vacuum behavior in quantum chromodynamics II, Phys. Rev. D **22**, 2022 (1980).

[23] K. Osterloh, M. Baig, L. Santos, P. Zoller, and M. Lewenstein, Cold atoms in non-Abelian gauge potentials: From the Hofstadter 'moth' to lattice gauge theory, Phys. Rev. Lett. **95**, 010403 (2005).

[24] J. Ruseckas, G. Juzeliūnas, P. Oehberg, and M. Fleischhauer, Non-Abelian gauge potentials for ultra-cold atoms with degenerate dark states, Phys. Rev. Lett. **95**, 010404 (2005).

[25] N. Goldman, A. Kubasiak, P. Gaspard, and M. Lewenstein, Ultracold atomic gases in non-Abelian gauge potentials: The case of constant Wilson loop, Phys. Rev. A **79**, 023624 (2009).

[26] E. I. Rashba, Fiz. Tverd. Tela (Leningrad) **2**, 1224 (1960) [Sov. Phys. Solid State **2**, 1109 (1960)]; Yu. L. Bychkov and E. I. Rashba, Oscillatory effects and the magnetic susceptibility of carriers in inversion layers, J. Phys. C **17**, 6039 (1984).

[27] G. Dresselhaus, Spin-orbit coupling effects in zinc blende structures, Phys. Rev. **100**, 580 (1955).

[28] B. Estienne, S. Haaker, and K. Schoutens, Particles in non-Abelian gauge potentials: Landau problem and insertion of non-Abelian flux, New J. Phys. **13**, 045012 (2011).

[29] Y. Li, S. C. Zhang, and C. Wu, Topological insulators with SU(2) Landau levels, Phys. Rev. Lett. **111**, 186803 (2013).

[30] Y. Li and C. Wu, High-dimensional topological insulators with quaternionic analytic Landau levels, Phys. Rev. Lett. **110**, 216802 (2013).

[31] Y. Li, K. Intriligator, Y. Yu, and C. Wu, Isotropic Landau levels of Dirac fermions in high dimensions, Phys. Rev. B **85**, 085132 (2012).

[32] M. F. Wondrak, W. D. van Suijlekom, and H. Falcke, Gravitational pair production and black hole evaporation, Phys. Rev. Lett. **130**, 221502 (2023).

[33] M. P. Hertzberg and A. Loeb, Inconsistency with de Sitter spacetime of "Gravitational Pair Production and Black Hole Evaporation", arXiv:2307.05243.

[34] M. N. Chernodub, Conformal anomaly and gravitational pair production, arXiv:2306.03892.

[35] S. C. Zhang and J. p. Hu, A four-dimensional generalization of the quantum Hall effect, Science **294**, 823 (2001); D. Karabali and V. P. Nair, Quantum Hall effect in higher dimensions, Nucl. Phys. **B641**, 533 (2002); K. Hasebe and Y. Kimura, Dimensional hierarchy in quantum Hall effects on fuzzy spheres, Phys. Lett. B **602**, 255 (2004); Ü. H. Coşkun, S. Kürkçüoğlu, and G. C. Toga, Quantum Hall effect on odd spheres, Phys. Rev. D **95**, 065021 (2017).

[36] K. Hasebe, Split-Quaternionic Hopf map, quantum Hall effect and twistor theory, Phys. Rev. D **81**, 041702 (2010).

[37] E. Jaynes and F. Cummings, Comparison of quantum and semiclassical radiation theories with application to the beam maser, Proc. IEEE **51**, 89 (1963).

[38] F. Haldane, Fractional quantization of the Hall effect: A hierarchy of incompressible quantum fluid states, Phys. Rev. Lett. **51**, 605 (1983).

[39] A. P. Balachandran, S. Kürkçüoğlu, and S. Vaidya, *Lectures on Fuzzy and Fuzzy SUSY Physics* (World Scientific, Singapore, 2007).